NOVA SCHOOL OF SCIENCE & TECHNOLOGY

DEPARTAMENT OF

Ciências da Vida

Patrícia Alexandra Lopes Nascimento

BSc in Biochemistry

Sacsin deletion disrupts Golgi organization and Autophagy in C6 rat glioblastoma cells

MASTER IN GENÉTICA MOLECULAR E BIOMEDICINA

NOVA University Lisbon

September, 2022

Sacsin deletion disrupts Golgi organization and Autophagy in C6 rat glioblastoma cells

Agradecimentos

Quero agradecer a todas as pessoas que estiveram envolvidas neste projeto. Começo por agradecer ao meu orientador Federico Herrera por me dar esta oportunidade e pela sua paciência e ajuda. Agradeço também a Fernanda Murtinheira por me guiar e pela sua grande ajuda. Por fim, quero agradecer à minha coorientadora Margarida Castro Caldas, aos meus colegas do laboratório "Cell Structure and Dynamics" e aos meus pais e família pelo seu apoio.

Abstract

Autosomal recessive spastic ataxia of Charlevoix-Saguenay (ARSACS) is a rare childhood-onset ataxia characterized by progressive cerebellar ataxia, spasticity, motor sensory neuropathy and axonal demyelination. ARSACS is caused by mutations in the SACS gene, which leads to the production of defective forms of the 520 kDa multidomain protein sacsin. C6 rat glioblastoma cells were targeted for sacsin deletion by means of CRISPR/Cas9 technique to generate an astroglial model of ARSACS. Sacsin knockout cell lines were isolated by Flow Cytometry-assisted Cell Sorting and sacsin loss was subsequently confirmed in further experiments. Intermediate filaments (IF) expression levels were analyzed upon serum starvation and incubation with IL-6 and BMP2 cytokines, while IF aggregation and their disruption on organelle organization was observed by immunocytochemistry. C6 SACS-/- cells revealed an increase in expression of IF proteins and aggregation of nestin in the juxtanuclear area. Golgi apparatus was often pushed out of the perinuclear area and disarrayed in SACS-/- cells. STAT3 and SMAD1/5 signalling was altered in C6 SACS-/- cells in response to cytokines. The expression of the alarmin protein S100B was significantly higher in C6 SACS-/- cells. The expression of the cytosolic form of the autophagy protein LC3-I was identical in both cells lines but the levels of the activated LC3-II form was reduced in C6 SACS-/- cells, indicating alterations in the autophagy flux. ER stress pathways were also analyzed for possible novel phenotypes in ARSACS cells. The expression of the Unfolded Protein Response (UPR)-related protein Bip did not differ for both C6 strains. CHOP had an increased expression in reference C6 cells in normal conditions but was unexpectedly not expressed in conditions of serum starvation. Withaferin A (WFA), a drug known to bind and disorganize the type III IF vimentin, disrupted Nestin filaments and induced Golgi dispersion similar to C6 SACS-/- cells. In conclusion, lack of sacsin protein disrupts glial intermediate filament assembly and intracellular organelle distribution, enhances S100B expression and impairs autophagy, while being inconclusive regarding ER stress. These results suggest a potential function for sacsin in glial cells and may have implications for treating ARSACS as well as a variety of human illnesses caused by the disruption of intermediate filament networks.

Keywords: ARSACS, Sacsin, C6 cells, Golgi, Autophagy

Resumo

A ataxia espática autossómica recessiva de Charlevoix-Saguenay (ARSACS) é uma ataxia rara com início na infância caracterizada por ataxia cerebelar progressiva, espasticidade, neuropatia sensório-motora e desmielinização axonal. ARSACS é causada por mutações no gene SACS, que leva à truncação da proteína sacsina multidomínio de 520 kDa. Células C6 de glioblastoma de rato foram selecionadas para deleção de sacsina através da técnica de CRISPR/Cas9 para produzir modelos de ARSACS de astroglia. Linhas celulares de knockout de sacsina foram isoladas através de Citometria de Fluxo-assisted Cell Sorting e a perda de sacsina foi posteriormente confirmada. Os níveis de expressão e a organização de filamentos intermédios (IF) foram analisados em condições de inanição de nutrientes e indução de citoquinas IL-6 e BMP2, enquanto a agregação de IF e a consequente disrupção da organização dos organelos foi observado por imunocitoquímica. Expressão elevada de proteínas de IF e agregação de nestina na posição juxtanuclear rodeado de Golgi disperso foi revelada em células C6 SACS-/-. A sinalização de STAT3 e SMAD1/5 demonstrou alterado em células C6 SACS-/-. A expressão da alarmina S100B revelou-se significativamente elevada nas células SACS-/-. A expressão da LC3-I citosólico foi idêntica em ambas linhas celulares, mas a forma ativada LC3-II presente em autofagosomas encontrou-se reduzido nas células C6 SACS-/-, revelando alterações no fluxo autofágico. Stress de ER foi analisado para possíveis fenótipos em modelos celulares ARSACS. A expressão de Bip relacionada com Resposta de Proteína Desdobrada (UPR) não diferiu em ambas linhas celulares. A expressão da proteína CHOP é superior em C6 controlo em condições normais, mas não foi expressa em testes de inanição. Withaferina A (WFA), uma droga conhecida por se ligar e desorganizar a proteína IF tipo III vimentina, perturbou os filamentos de Nestin e induziu a dispersão de Golgi, fenótipos semelhantes a modelos celulares ARSACS. Concluindo, a falta de sacsina causa a disrupção de IF em células gliais e na organização de organelos intracelulares, aumenta a expressão da S100B e prejudica a autofagia, apesar de ser inconclusivo no que diz respeito à neuroinflamação e ao stress ER. Estes resultados sugerem uma função potencial para a sacsina em células glial e podem ter implicações no tratamento de ARSACS, bem como uma variedade de doenças humanas causadas pela perturbação das redes de filamentos intermédios.

Termos – chave: ARSACS, Sacsin, células C6, Golgi, Autofagia

Index

List of Tables

List of Figures

List of Abbreviations

AD – Alzheimer's disease

ALS – Amyotrophic lateral sclerosis

ARSACS - Autosomal recessive spastic ataxia of Charlevoix-Saguenay

BiP – Binding immunoglobulin protein

BMP - Bone morphogenetic protein

BSA – Bovine Serum Albumin

CAMs - CNS-associated macrophages

Cas9 - CRISPR-associated protein 9

Cav-1 - caveolin-1

CCL19 - Chemokine (C-C motif) ligand 19

CCL21 - Chemokine (C-C motif) ligand 21

CHOP - C/EBP Homologous Protein

CNS – Central nervous system

Co-SMAD – Co-mediator SMAD

CREB - cAMP-response element binding protein

CRISPR - Clustered regularly interspaced short palindromic repeats

CRP - C-reactive protein

CXCL12 - CXC chemokine

DA neurons - Dopaminergic neurons

DEPs – Differentially expressed proteins

DMEM – Dulbecco's Modified Eagle Medium

DMSO – Dimethylsulfoxide

DPBS – Dulbecco's phosphate buffered saline

Drp-1 – Dynamin-related protein 1

ECL – Enhanced chemiluminescence

EDTA – Ethylenediamine tetraacetic acid

EGFP - epidermal growth factor receptor

ER – Endoplasmic reticulum

ERAD - ER-associated degradation

ERK – Extracellular signal-regulated kinases

FACS – Flow Cytometry-assisted Cell Sorting

FBS – Fetal Bovine Serum

FCCP - reversible inhibitor of mitochondrial oxidative phosphorylation

FTCD - formiminotransferase cyclodeaminase

GA - Golgi apparatus

GAP-43 - growth-associated protein 43

GAPDH – Glyceraldehyde 3-phosphate dehydrogenase

GFAP – Glial fibrillary acidic protein

GFP – Green fluorescent protein

Gp130 – Glycoprotein 130

GTP - Guanosine-5'-triphosphate proteins

HAD - HIV-1 associated dementia

HDFs - Human dermal fibroblasts

HEPN - higher eukaryotes and prokaryotes nucleotide-binding

HSP – heat shock proteins

IFs – Intermediate filaments

IL – interleukin

IL-6 – Interleukin 6

IL-6R – Interleukin 6 receptor

IRE-1 – Inositol-requiring enzyme 1

I-SMADs – Inhibitory SMADs

JAK – Janus kinase

KO – Knockout

LC3 - 1A/1B-light chain 3

LIF - Leukemia inhibitory factor

MS – Multiple sclerosis

NF-kB – Nuclear factor kappa-light-chain-enhancer of activated B cells

PD - Parkinson's disease

PE - phosphatidylethanolamine

PERK – Protein kinase RNA-like ER kinase

PI3K - phosphatidylinositol-3-kinase

PKC - protein kinase C

RAGE - receptor for advanced glycation end products

ROS - Reactive oxygen species

RSK - Ribosomal s6 kinase

R-SMADs – Receptor-regulated SMADs

S100B -S100 calcium-binding protein B

SACS - Sacsin Molecular Chaperone

sALS - sporadic amyotrophic lateral sclerosis

SBE - SMAD-responsive promoter

SDS – Sodium dodecyl sulphate

SDS-PAGE – Sodium dodecyl sulphate–polyacrylamide gel electrophoresis

SIRPT – Sacsin internal repeated regions

SMAD – Drosophila gene 'mothers against decapentaplegic' (Mad) and C. elegans gene Sma

SNAREs - soluble N-ethylmaleimide-sensitive factor attachment protein receptors

SOCS3 - Suppressor of cytokine signaling 3

SRR – Sacsin repeated regions

STAT3 – Signal transducer and activator of transcription 3

SVZ - subventricular zone

TBS – Tris-buffered saline

TBS-T – tris-buffered saline-tween 20

TGF – β - anti-inflammatory transforming growth factor β

TGF-β – Transforming growth factor beta

TNF – Tumour necrosis factor

Ube3A ubiquitin protein ligase

UPR - unfolded-protein response

WFA – Withaferin A

XPCB - xeroderma pigmentosum complementation group C binding

Introduction

1. ARSACS

The second most common ataxia, autosomal recessive spastic ataxia of Charlevoix-Saguenay (ARSACS), is a rare childhood-onset neurodegenerative disorder that was first discovered in the regions of Charlevoix and Saguenay-Lac-et-Sant of Quebec, Canada. ARSACS´ higher frequency in that region is due to a founder effect. Common clinical features of ARSACS are cerebellar ataxia, pyramidal spasticity, motor sensory neuropathy with variable intellectual dysfunction, axonal demyelination, and retinal changes[1, 2].

More than 200 mutations in the SACS gene (chromosome 13q12) have been linked to ARSACS[1]. This gene encodes for the 520 kDa protein sacsin composed of 4,579 amino acids[3], which function is still largely unknown due in part to the gene's and protein's enormous size, which makes research into this disease difficult. Sacsin contains a ubiquitin-like domain at the N-terminus capable to bind to the proteosome known as ubiquitin-like (Ubl) domain and a xeroderma pigmentosum complementation group C binding (XPCB) domain that binds to the Ube3A ubiquitin protein ligase[2]. In the C-terminus, Sacsin has a DnaJ domain, which is able to bind to the Hsc70 heat shock system and a higher eukaryotes and prokaryotes nucleotide-binding (HEPN) domain that mediates sacsin's own dimerization and binding to nucleotides.[2, 4–6] The largest fraction of the protein is occupied by three large internal repeats sequences named "sacsin repeat regions" (SRRs), that may have a Hsp90-like chaperone function[2]. SRRs are formed by the sequence repeats SIRPT1, SIRPT2 and SIRPT3, each containing tree subrepeats sr1, sr2 and sr3. These large repetitions encompass 84 percent of the gene and are conserved in vertebrate mammals. The structural features of sacsin and a few reports indicate that sacsin has a co-chaperone function.

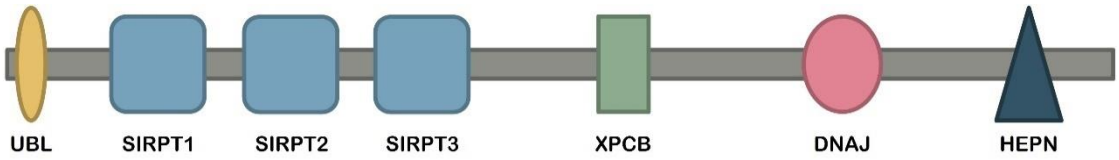

Figure 1 – Sacsin primary domains.

The loss of sacsin has demonstrated cytoskeleton and mitochondrial disruption in ARSACS cellular and mice models. Although Sacsin is expressed in all regions of the brain, Purkinje cells have the highest levels of SACS mRNA and sacsin expression, which is consistent with the Purkinje cell degeneration characteristic of ARSACS. Neurofilament accumulation in the absence of the sacsin protein is a known phenotype in neuronal cell population in ARSACS patients and in ARSACS mice[2]. Bundling and collapse of the vimentin intermediated filament (IF) system was also observed in cultured fibroblasts from ARSACS patients[2, 7], suggesting a role of sacsin in IF assembly and maintenance[1]. Other cellular alterations include subcellular reorganization of

proteostasis system components, altered autophagy and abnormalities in organelle distribution, such as fragmentation of the Golgi, asymmetrical positioning of nuclei and displacement and morphological changes of mitochondria in sacsin knockout neurons[3]. The morphological changes in mitochondria are consistent with the alterations in the function of the fission factor dynamin related protein 1 (Drp1), and lead to impaired oxidative phosphorylation and oxidative stress[2]. These phenotypes could be related to IF network disruption: the cytoskeleton is critical for mitochondrial dynamics.

Understanding how the absence of sacsin affects the intricate and well-ordered process of IF formation could provide insight into the cellular pathophysiology of ARSACS. The cytoskeleton is a complex network of filamentous proteins important to control the viscoelastic properties and mechanical strength of cells, organize and give structure to their interior, and control many dynamic processes, such as intracellular trafficking, cell division, adhesion, and locomotion[8, 9]. There are three types of fiber protein systems: Actin/myosin microfilaments, microtubules and intermediate filaments (IF)[8, 9]. They are interconnected with linker proteins, such as plectin, that establishes cross-links between IFs, microtubules and actin filaments[8]. The IF family consists of diverse filamentous cytoplasmatic proteins originated from a divergence of the nuclear intermediate filaments Lamins[10], which are ubiquitously expressed and highly conserved during evolution[9]. IFs are responsible for providing structural stability of the cell, spanning from the nucleus to the cell membrane, and to transduce biochemical and mechanical signals into biological responses[9, 11]. IF are subdivided in six classes of proteins. Type I and II of the IF family comprises the acidic and basic keratins, respectively[10]. The type III proteins include Vimentin, Desmin and GFAP, able to homopolymerize and heteropolymerize with each other[10]. Type IV consists of Nestin, neurofilaments and synenins, manly expressed in neurons and muscle, These are the only IFs that polymerize exclusively by forming heterodimers and heterotetramers with other types of IF proteins, specially type III, such as Vimentin and glial fibrillary acidic protein (GFAP)[10]. Type V are the Lamins, the nuclear intermediate filament proteins. Type VI are lens-specific beaded intermediate proteins: phakinin (CP49) and filensin[10]. Types III and IV, particularly Vimentin, GFAP and Nestin, are the IF proteins known to be affected from the loss of sacsin and, therefore, the IF proteins used for this thesis' analysis.

Vimentin is a specific marker for astrocytes and ependymal cells in glial precursors, becoming an early marker of glial differentiation because it is expressed before the onset of GFAP expression[12], which is a predominant IF protein in astroglia[11]. Nestin is mostly expressed in neurons and muscle cells but also highly expressed in astrocytes[10, 13]. Both Nestin and GFAP are known to have increased expression during pathological situations: Nestin helps the formation of the glial scar after CNS injury[14], while GFAP is induced not only by acute brain injury but also by chronic pathology, such as Alzheimer disease or non-specific gliosis[15]. Disorders with IF pathology

include neurodegenerative disorders, myopathies, cataracts, skin conditions, and sensorimotor neuropathies, among others [1]. Since IF disruption is a common phenotype in ARSACS cells, understanding how sacsin regulates IF protein assembly is essential to understanding sacsin's function. IF-disruption reagents like Withaferin A (WFA)[10, 16], that binds to the cysteine-328 in the helix termination or 2B region of the α-helical central rod domain of vimentin[16], can help researchers uncover the mechanism of IF assembly by sacsin by examining the functions of IF assembly, maintenance, and stability[10].

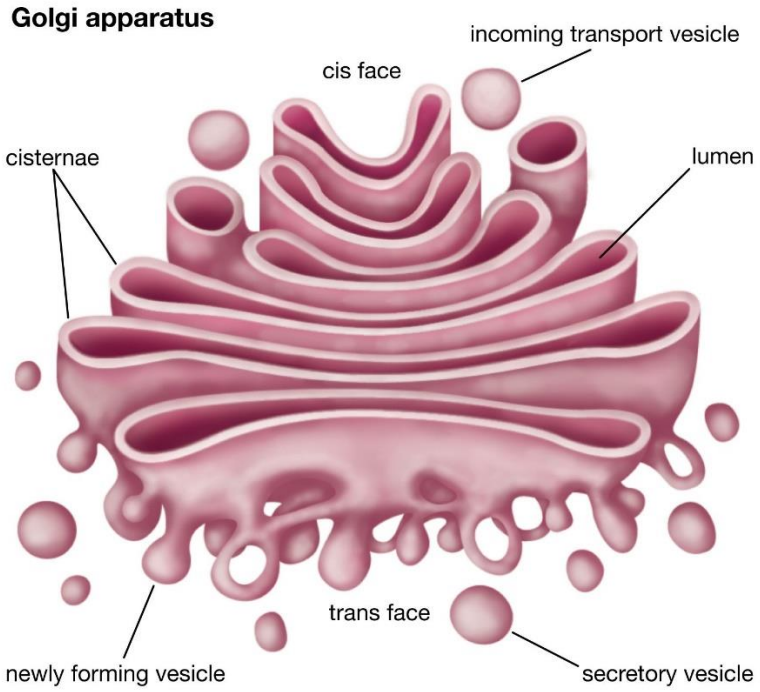

Figure 2 – The Golgi Apparatus structure. The Golgi apparatus, or complex, plays an important role in the modification and transport of proteins within the cell. Source: Rogers, K.

The disruption of the cytoskeleton network often compromises the positioning and function of organelles. The Golgi apparatus (GA) is responsible for transport, processing and sorting of proteins that are synthesized in the rough endoplasmic reticulum (ER)[17]. GA is composed of parallel opposite cisternae that function as ports of transport vesicles through coordinated fission of vesicles from one cisterna's lateral edge and fusion to the next cisterna[17] (Figure 2). GA structural and functional integrity is conserved by joint coordination of microtubules and associated proteins, actin cytoskeleton, the Golgi matrix proteins, and proteins that regulate the targeting and fusion of transport vesicles, such as GTP-binding proteins and SNARES[17]. Moreover, GA binds to vimentin with the formiminotransferase cyclodeaminase (FTCD), indicating that vimentin is involved in the Golgi apparatus' placement[18, 19]. Fragmentation and dispersion of GA was shown in a variety of neurodegenerative diseases, but was first reported in sporadic amyotrophic lateral sclerosis (sALS)[20, 21]. Similar features were found in Alzheimer’s

disease (AD), in corticobasal degeneration and in the ballooned neurons in Creutzfeldt-Jacob disease[17]. Human dermal fibroblasts (HDFs) from ARSACS patients had Golgi fragmentation caused by the aggregation of IF cytoskeleton[2]. In this thesis, both the aggregation of IF cytoskeleton and their effects on GA organization were analyzed and studied on glial cell model of ARSACS and we confirmed that the loss of sacsin can affect glial cells just as neurons.

Most studies about ARSACS focus solely on neurons, neglecting the contribution of glial cells, such as astroglia or microglia. Both are important for maintaining the neuronal environment within the Central Nervous System (CNS), and establish complex interactions with neurons [22]. Microglial cells, derived from yolk-sac primitive myeloid progenitor cells, are resident immune cells and phagocytes of the CNS, together with the non-parenchymal perivascular, meningeal, and choroid plexus macrophages, referred as CAMs (CNS-associated macrophages), who are responsible for the immunological barrier at CNS interface[23, 24]. In a stable and healthy state, microglia carry out a dynamic surveillance and maintenance of the CNS microenvironment, modulating synaptic plasticity and removing dead cells[22]. However, in a diseased brain, microglia are key players in neuroinflammation.[25] While microglial cells have an overall protective role against CNS insults, sustained inflammation can lead to deleterious effects[22].

Astrocytes are star-shaped cells with a complex and heterogeneous morphology in various locations in the CNS, previously distinguished as fibrous or protoplasmic astrocytes found in the white and grey matter, respectively[22]. Currently, a more accurate nomenclature categorizes the anatomical diversity of astrocytes in a wider range of subtypes, such as the cerebellar Bergmann glia, the retinal Muller cells, the pituitary astrocytes pituicyte, the subventricular zone (SVZ) astrocytes and those forming the blood-brain-barrier[26]. Astrocytes, together with neurons and oligodendrocytes, are developed from radial cells, which are derived from neuroepithelial stem cells. Starting from the ventricular zone, astrogenesis begins in mid-embryogenesis and continues postnatally until the astrocytes migrate and mature through the CNS[22, 26]. These glial cells contribute to the neural circuits, maintain homeostasis, provide help to neurons during synaptic signaling and respond to stress and injury. Astrogliosis is the body's reaction to neurological conditions like trauma, inflammation, or neurodegeneration in order to shield the CNS from injury and to repair damaged neurons[22]. GFAP, the main intermediate filament (IF) of the astrocytes, is upregulated during astrogliosis and is a well-known hallmark of reactive astrocytes[22].

2. Neurodegenerative phenotypes and altered systems in the cell

Neurodegenerative diseases may be defined by a specific altered protein, but these diseases share a list of common pathophysiological mechanisms associated with progressive neuronal dysfunction and death, namely proteotoxic stress and its attendant abnormalities in ubiquitin–proteasomal and autophagosomal/lysosomal systems, oxidative stress, mitochondrial stress, DNA damage, dysregulation of neurotrophins, programmed cell death, and neuroinflammation[27, 28]. Studies with ARSACS fibroblasts confirmed enhanced autophagy[2, 29, 30], and analysis of ARSACS mice models and isolated patient cells revealed multiple impaired pathways and differentially expressed proteins (DEPs) connected with neuroinflammation, synaptogenesis, or cell engulfment[31, 32].

2.1. Neuroinflammation

Neuroinflammation is a natural defensive response against brain or spinal cord injury or viral/bacterial infections[28]. This response is in principle beneficial, promoting tissue repair and removal of cellular debris, but sustained inflammation is detrimental an inhibits tissue regeneration[28]. This chronic inflammation is a consequence of endogenous (genetic mutation and protein aggregation) or environmental (infection, trauma, and drugs) factors, usually involving microglia and astrocytes and playing a key role in many neurodegenerative diseases[28].

2.1.1. IL-6/STAT3 pathway

Neuroinflammation is regulated by pro-inflammatory cytokines (e.g. tumor necrosis factor (TNF)-α, interleukin (IL)-1, IL-6, and IL-12) and anti-inflammatory cytokines (e.g. bone morphogenetic protein 2 (BMP-2)), chemokines (e.g. CCL19, CCL21 and CXCL12)[33], second messengers (e.g. nitric oxide and prostaglandins), and reactive oxygen species (ROS)[34]. IL-6 is a pro-inflammatory cytokine with a pleiotropic activity that triggers the synthesis of acute phase proteins in hepatocytes, including C-reactive protein (CRP), serum amyloid A, fibrinogen, and hepcidin[35]. IL-6 binds to transmembrane class I cytokine IL-6 receptors (IL-6R) with no intrinsic enzymatic activity[36]. Instead, they recruit dimers of the gp130 co-receptor , which is dimerized[37], leading to the activation of the Janus kinase (JAK) family. JAK family proteins are involved in several pathways such as phosphatidylinositol-3-kinase (PI3K), extracellular signal-regulated kinase (ERK), mitogenactivated protein kinase and signal transducer and activator of transcription 3 (STAT3) pathways[38].

The STAT family is comprised of seven functionally and structurally similar proteins STAT1, STAT2, STAT3, STAT4, STAT5a, STAT5b, and STAT6. STAT family is responsible for regulation of gene transcription related to cell cycle, cell survival, and immune response[39]. When induced by IL-6, STAT3 is phosphorylated by JAK kinase in tyrosine 705 (Y705) residue[39],

leading to homodimerization of two STAT3 through the interaction of p-Tyr705 of one monomer with the p-Tyr705 of another. When the active dimer separates from the receptor, it migrates from the cytoplasm to the nucleus, where it binds to certain DNA sequences and triggers transcription[39] (Figure 3).

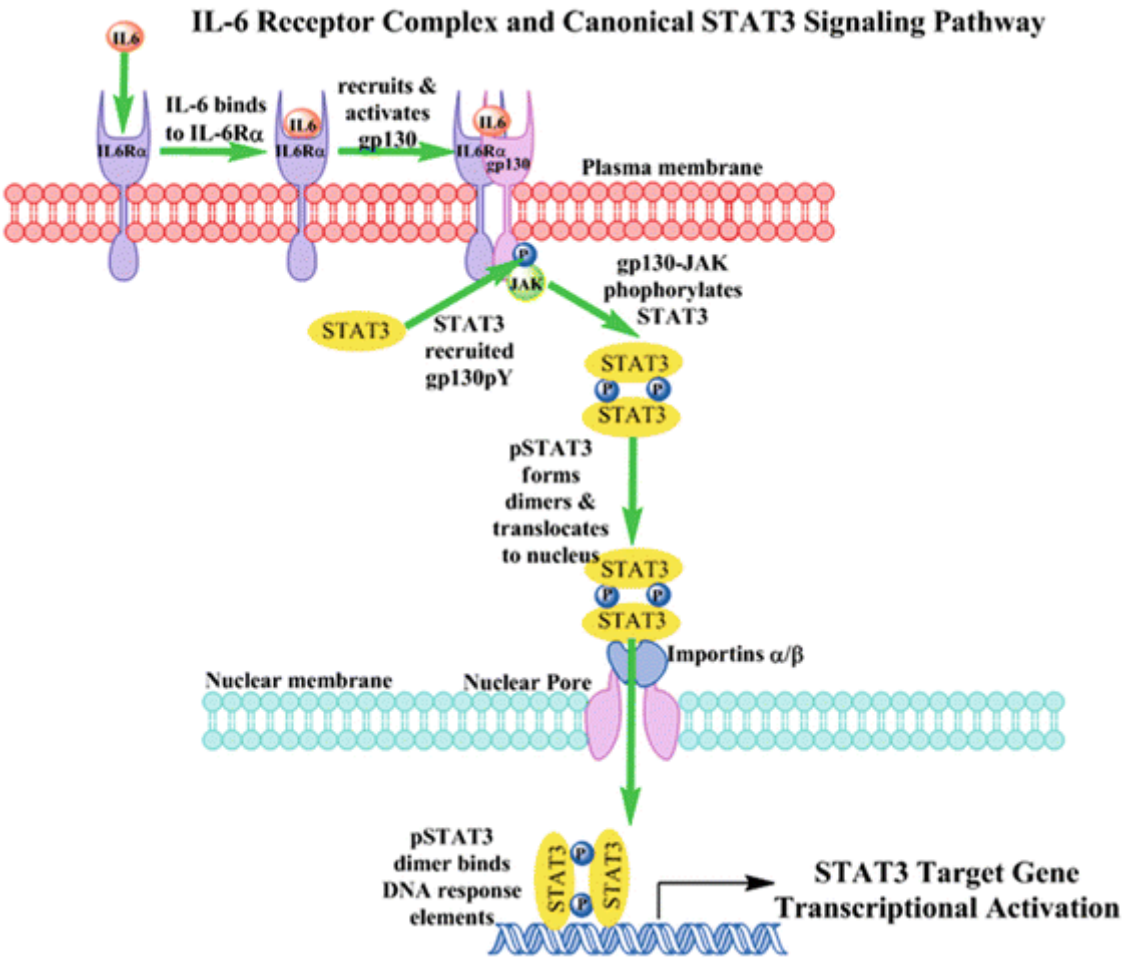

Figure 3 – IL-6/STAT3 pathway. Interleukin-6 initially interacts with and binds to IL-6-receptor-subunit (IL-6R) in the plasma membrane of cells. Latent STAT3 is recruited to certain pY docking sites on the gp130 subunits of active receptor complexes. The associated JAK of the activated IL-6 receptor complex phosphorylates STAT3 at pY705. The nuclear pore complex is the only entry point for large protein complexes like pSTAT3-Y705 dimers. Source: Johnston, P.A.

STAT3 is highly expressed in the peritoneum, leukocytes in the peripheral circulation, and neutrophils in the bone marrow, as well as the peripheral nervous system and digestive tract[39]. STAT3 mutations cause autosomal dominant hyperimmunoglobulin E syndrome (HIES), which manifests as recurring bacterial infections of the skin and lungs, increased oral fungal infection, elevated innate immune pro-inflammatory responses, bone and connective tissue abnormalities, and increased circulating immunoglobulin E. (IgE)[40]. When mice bearing mutant STAT3 were transplanted with STAT3-sufficient hematopoietic cells, the proper inflammatory and immunological responses were restored[40], demonstrating the relevance of STAT3 in mediating

inflammation. STAT3 is overexpressed or constitutively active in 70% of human solid and hematological tumors, where it plays a key role in cancer cell proliferation and survival[39]. Chronic brain inflammation is a major factor in neurodegenerative conditions, where the highly concentrated/expressed IL-6 causes overexpression and abnormal activation of STAT3 in AD, HIV-1 associated dementia (HAD), multiple sclerosis, and Parkinson's disease (PD) that accelerate the deterioration of the central nervous system[41–43].

2.1.2.BMP2/SMAD pathway

The BMP-SMAD pathway has an important role during embryonic development and is one of the major pathways for controlling neurogenesis in post-natal nerve tissue regeneration and repair[44, 45]. BMP cytokines belong to the anti-inflammatory transforming growth factor β (TGF - β) superfamily and are multifunctional cytokines that control cell growth and differentiation, chemotaxis, and apoptosis[45]. BMP cytokines bind to transmembrane serine/threonine kinase receptors BMPR, forming a heterodimeric complex of type I and type II kinase receptors and starting a signal transduction cascade. BMPR then recruits and phosphorylates the C-terminus receptor-regulated SMADs (R-SMADs), such as SMAD1, SMAD5 and SMAD8[46, 47]. Activated transcriptional factors R-SMADs binds to the co-SMAD (SMAD4) to translocate to the nucleus. Coactivators and Inhibitory SMADs (I-SMADs), localized in the nucleus, associate with the complex R-SMAD and SMAD4 to regulate gene expression[45, 48]. SMAD7 is a suppressor of TGF-β/SMAD pathway by binding to TGF-b receptors and preventing R-SMADs phosphorylation[48, 49].

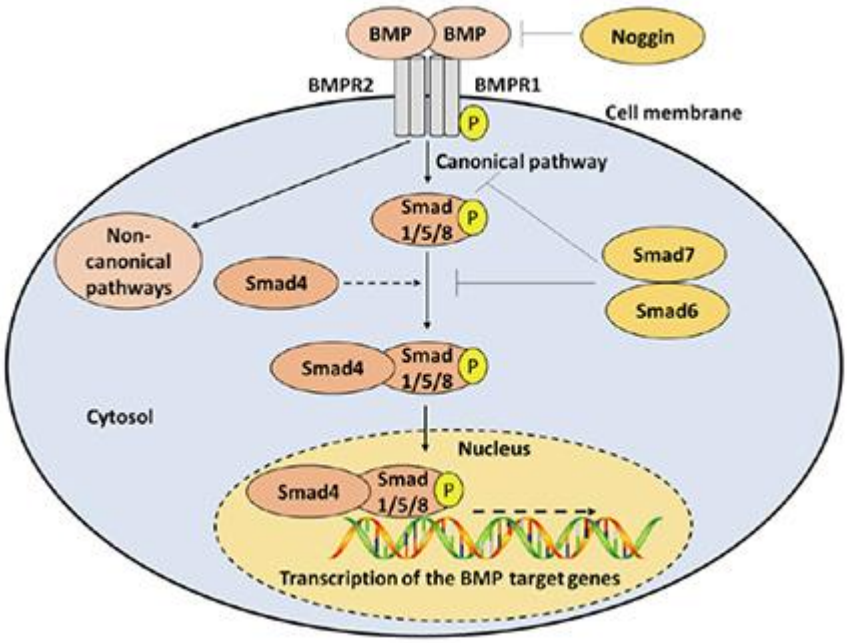

Figure 4 - BMP signaling pathways. Bone morphogenic protein: BMP; BMP receptor: BMPR. Source: Al-Sammarraie, N.

During primary embryonic development, both IL-6 cytokines and BMP-2 induce astrocyte differentiation in synergy[50]. STAT3 and SMAD1 form a complex with transcriptional coactivator p300: STAT3 binds in a cytokine-independent manner at the C-terminal of p300, while SMAD1 binds at the N-terminal in a cytokine-dependent manner[50]. This complex plays a role in the cooperative signaling of LIF and BMP-2 and the consequent development of astrocytes from neural progenitors[50, 51]. However, TGF-β therapy suppresses delayed phase gene expression that was increased by IL-6. STAT3 and SMAD proteins could work in opposition to each other in the setting of inflammation since TGF-β is an anti-inflammatory cytokine[52] while IL-6 and other cytokines that activate STAT3 are pro-inflammatory[53].

A deficit in BMP function typically results in pronounced abnormalities or serious diseases because of their significance as regulators of many genes throughout the body. For instance, in mouse models, lack of BMP function is associated with neurological abnormalities[54]. The differentiation of certain neuron classes by BMP12 signaling in the spinal cord suggests that BMPs have a role in defining the identity of neurons in the central nervous system. In AD, an aberrant number of phosphorylated SMAD2 is localized in the cytoplasm in pyramidal neurons of the hippocampus. However, SMAD7 is overexpressed due to aberrant concentration of amyloid-β (Aβ) in AD cells, suppressing the TGF-β signaling. This proposes a disruption in the TGF-β/SMAD signaling pathway, which may result in a reduction or loss of TGF-β's neuroprotective effects, potentially accelerating neurodegeneration[49]. Downregulation of the BMP/SMAD pathway in Parkinson's disease was also found: inhibitory SMAD6 is upregulated in the substantia nigra[55]. Studies on the role of BMP-SMAD signaling pathway on ARSACS are still lacking.

2.1.3.S100B

An increase in gene expression of the S100B protein in astrocytes and oligodendrocytes in neurodegenerative diseases led to its use as a surrogate marker for the diagnosis or prognosis of neurodegeneration[56]. However, there are still no studies about overexpression of S100B in ARSACS.

S100B belongs to the multigenic S100 family, constituted by ~10 kDa proteins with two calcium binding sites with helix-loop-helix (‘‘EF-hand type’’) conformations[56, 57]. At least 20 members of the S100 family are exclusively expressed in vertebrates. S100B is composed of S100 ββ homodimers and, more rarely, forms heterodimers of β subunits with S100 α1. S100B is involved in cell growth, interacting with growth-associated protein 43 (GAP-43), the regulatory domain of protein kinase C (PKC), the anti-apoptotic factor Bcl-2, the tumor suppressor protein p53[58] and the tau protein, among others. In fact, tau protein is a target of the S100B chaperone, which

suppresses tau protein aggregation and seeding in tau pathologies, namely frontotemporal dementia and parkinsonism associated to chromosome 17 (FTDP-17) and AD[59].

Besides intracellular processes, S100B is a secreted protein with cytokine activity[56]. It mediates communication among glial cells and between glial cells and neurons, by binding to the receptor for advanced glycation end products (RAGE), a multiligand receptor responsible for signal transduction of inflammatory, neurotrophic and neurotoxic stimuli[56, 60]. S100B has opposite effects depending on its concentration: nanomolar concentrations promote neurite growth and neuronal survival; while micromolar concentrations induce neuronal apoptosis, and production of pro-inflammatory cytokines[56, 61]. However, high expression of S100B blocks CREB phosphorylation and inhibits IL6/STAT3-signaling in malignant melanoma cells. S100B also binds to and sequesters ribosomal S6 kinase (RSK) by blocking its phosphorylation at T573. CREB phosphorylation in the nucleus is blocked by S100B-RSK complex, leading to a decrease of CREB-dependent transcription of IL-6 and loss of IL-6/STAT3 signaling in melanoma[57]. S100B also interferes with the formation of IF protein filaments in a Ca^{2+} and dose-dependent manner when it is complexed with S100A1[58, 62]. It binds to the N-terminal of GFAP and prevents its phosphorylation in this region[58], which is essential for polymerization and filament assembly[58, 62]. The S100B and S100A1 complexes also influence vimentin in a similar manner, indicating that they interact and interfere with the assembly of vimentin monomers into intermediate filaments[58, 62].

2.2. Autophagy

Autophagy is a major system of elimination of long-lived proteins, protein aggregates and damaged organelles. Autophagy comprises two major steps: 1) Double-membraned autophagosomes are formed to engulf intracellular components and then 2) they are fused with lysosomes to form autolysosomes. In the lysosomes, the engulfed components are degraded by lysosomal hydrolases. The mechanism of autophagy is conserved to all species[63–65], and is essential for cellular recycling and protein homeostasis. This system is also responsible for cell survival during starvation, antigen presentation, viral and bacterial infection, and cell death. Autophagy dysfunction has been hypothesized as an underlying mechanism for cancer, hepatic inflammation, neurodegeneration and muscular diseases[63–65]. Fibroblasts from ARSACS patients show displacement of HSP70 and components of the autophagy–lysosome machinery, more concentrated in the juxtanuclear region of vimentin accumulation[2].

One of the key regulators of autophagy is the microtubule-associated protein 1A/1B-light chain 3 (LC3), that initiates the autophagosome biogenesis[63]. LC3 is a ~17kDa soluble protein present ubiquitously in the cytoplasm in the inactive form, LC3-I. LC3-I is then conjugated to phosphatidylethanolamine (PE) through two consecutive ubiquitylation-like reactions catalyzed

by the E1-like enzyme Atg7 and the E2-like enzyme Atg3[64] to form LC3-phosphatidylethanolamine conjugate (LC3-II) during the formation of autophagosomes. LCE-II is then degraded by the lysosomal proteases in the autolysosomes[63–65].

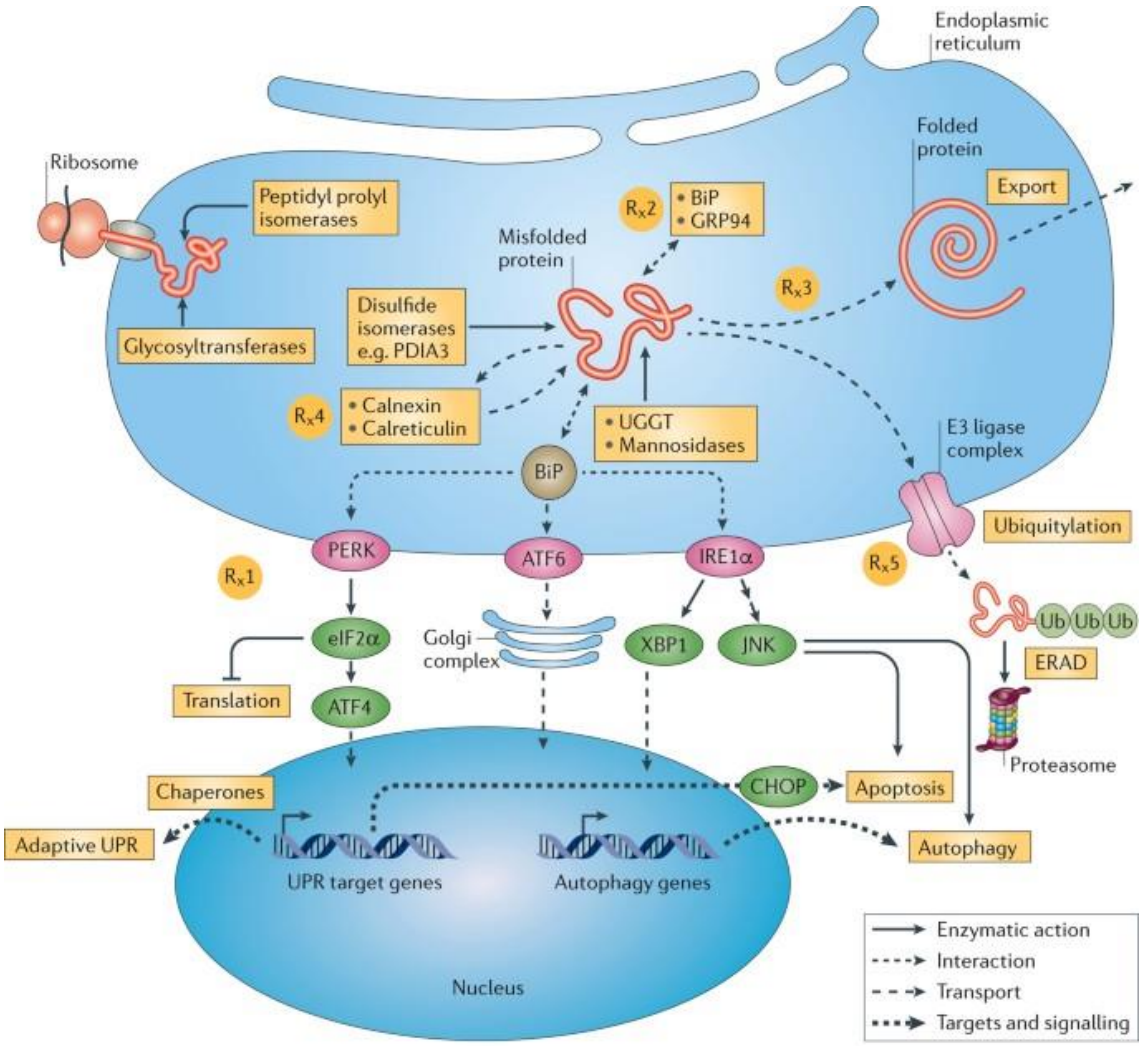

Figure 5 – Protein folding and activation of unfolded-protein response (UPR) in endoplasmic reticulum (ER). Proteins are translocated into the lumen of the ER after translation to attain their correctly folded conformation via folding enzymes. Adaptive UPR is initiated by activation of three protein sensors, activating transcription factor 6 (ATF6), inositol-requiring enzyme 1α (IRE1α) and PRKR-like ER kinase (PERK). BiP dissociates from the sensors, and interacts with the misfolded proteins. The downstream effects may include gene transcription and inhibition of translation (adaptive UPR), induction of autophagy or apoptosis, or ER-associated degradation (ERAD). Source: Cybulsky A. V.

2.3. Increased ER stress

Neurodegenerative diseases often show impairments in the function of the endoplasmatic reticulum (ER). ER stress is often observed due to the aggregation and accumulation of unfolded proteins in the ER[66, 67]. This leads to induction of the unfolded-protein response (UPR) activated by the type-I transmembrane protein kinase, IRE1, and PKR-like endoplasmic reticulum kinase (PERK) in response to still unknown signals[66, 67]. These two transmembrane proteins will dissociate from Bip[67], agglomerate and induce the transcription of genes involved in stress responses, amino acid metabolism, redox reactions, protein folding, processing, secretion and degradation, ER-associated degradation (ERAD), autophagy, mitophagy and apoptosis[68] (Figure 5). CHOP is the main protein that induces ER stress-related apoptosis when the damage cannot be repaired to maintain tissue homeostasis[66]. ER stress and deregulation of the UPR response is one of the symptoms of neurodegenerative diseases: CHOP is often found upregulated in Parkinson, Alzheimer's, and Huntington's diseases, and in type-I diabetes and brain ischemia[66]. ER stress-pathways have not been analyzed in detail in ARSACS, but the expression of the ER stress-related chaperone calreticulin is impaired in ARSACS patients' cells[4].

3. Aims

Astroglial-like C6 rat glioblastoma cells exhibit high quantities of sacsin protein. We have recently produced the first astroglial model of ARSACS by knocking sacsin out of these cells by means of CRISPR/Cas9. Although the importance of astroglia in ARSACS is still unknown, their key involvement in neurodegenerative and neurodevelopmental disorders is widely accepted. In this study, we sought to describe potential cellular and molecular alterations following sacsin deletion in astroglial-like C6 cells. The intermediate filament system and the organelle distribution, which is found altered in ARSACS neurons and fibroblasts, were our main focus of interest. Additionally, we looked into various markers for neuroinflammation, autophagy, and ER stress that are known to be impacted in other neurodegenerative disorders.

Methods

Reagents

Dulbecco's modified Eagle's medium (DMEM) was purchased from Biowest (Nuaillé, France); Fetal bovine serum (FBS), rotenone, dimethylsulfoxide (DMSO), were acquired from Sigma-Aldrich (St. Louis, MO, USA). Penicillin Streptomycin (Pen/Strep), Pierce ECL Plus Western Blotting Substrate, MitoTracker Red CMXRos and Hoechst 33342 were purchased from Invitrogen, Life Technologies (Carlsbad, CA, USA). Protease inhibitor cocktail was purchased from Abcam. Phosphatase inhibitor cocktail was purchased from NZYTech (Lisboa, Portugal). Interleukin-6 (IL-6) and the soluble IL-6 receptor (IL-6R) were obtained from R&D Systems (Minneapolis, MN, USA). Plasmids EYFP-Golgi7 and mDsRed-Golgi-7 were developed in Michael Davidson lab (Addgene plasmids # 56590 and # 55832. The LC3-EGFP-mCherry construct was a gift from Chiara Zurzolo (Institut Pasteur, Paris); The ER-DsRed plasmid was obtained from Jia-Yi Li Laboratory, Lund University. DsRed2-ER-5 was a gift from Michael Davidson (Addgene plasmid # 55836; http://n2t.net/addgene:55836; RRID: Addgene_55836).

Cell Culture and Treatments

C6 rat glioblastoma cells were acquired from ATCC (CCL-107™). This cell line was grown in DMEM medium supplemented with 10% v/v Fetal Bovine Serum (FBS) and 1% Penicillin and streptomycin mix and maintained at 37ºC in a 5% CO_2 atmosphere. C6 cells were plated on sterile plates or glass coverslips 16h-24h or 48h before experiments. For cytokine treatments, culture medium was removed, and cells were washed with PBS (Thermo Fisher Scientific; Waltham, MA, USA) and incubated with serum-free medium for 2h. Then, cells were incubated in serum-free medium with the following cytokines: IL-6/IL-6R (30 ng/mL), for 20 minutes or 24 hours; IL-11, IL-22, OSM, CNTF (30ng/mL), IFN- α (100ng/mL) for 30 minutes or 24 hours; BMP-2 (125ng/mL) for 2 hours.

To test the effect of starvation in intermediate filaments and ER stress-related proteins, cells were submitted to serum-free medium. Twenty-four hours after seeding, cells were washed with PBS and incubated with DMEM without FBS for 48h.

Cells were transfected 24h after seeding with plasmids expressing target proteins bound to fluorophores for Microscopy. Plasmids EYFP-Golgi7, mDsRed-Golgi-7, LC3-eGFP-mCHERRY, DsRed2-ER-5 were transfected in C6 and C6 $Sacs^{-/-}$ culture cells using JetPRIME transfection reagent (Polyplus transfection, Illkirch, France), at 1:2, 1:3 and 1:4 transfections ratios of DNA (µg): JetPRIME (µl) during optimization of transfection, concluding that 1:3 ratio was the most efficient. Eighteen hours after transfection, medium was replaced with DMEM with FBS for 2 hours before cell preparation due to the toxic effect inflicted on C6 from prolonged incubation

with JetPRIME reagent. In some experiments, cells were also incubated with different concentrations of WFA (10uM, 5uM, 2,5uM and 1uM) in 24 well plates together with EYFP-Golgi7 plasmid transfection and incubated during the same 18 hours of transfection.

Sacsin knockout cell line generation

C6 cells were transfected with the CRISPR/Cas9 KO plasmid (Santa Cruz Biotechnologies,Dallas, TX, USA) with the Jetprime transfection reagent in a ratio of 1µg of DNA to 3 µL of Jetprime and following manufacturer's instructions. Cells were sorted using the method BD FACSAria III (BD biosciences, Franklin Lakes, NJ, USA) after 24h hours transfection and GFP-positive cells were isolated and grown from single cells. Various clones were tested for their expression of sacsin, and one of them was chosen for subsequent studies. These tasks were previously performed by Fernanda Murtinheira, we just confirmed absence of sacsin in these cells.

Protein Extraction

Reference C6 and C6 SACS-/- cells were seeded at a concentration of 500 000 cells/mL with 1.5 ml of medium in 35mm dishes. Cells were then washed with DPBS (Cytiva; Marlborough, MA, USA) and lysed using NP-40 lysis buffer (150 mM NaCl, 50 mM Tris-HCl pH 7.4/7,5, 1% NP-40) or Native lysis buffer (150 mM NaCl, 50 mM Tris-HCl pH 7.4/7.5), both supplemented with protease inhibitors (Protease Inhibitor cocktail EDTA free, abcam, Cambridge, UK) and phosphatase inhibitors (Halt Phosphatase Inhibitor Single-use cocktail, Thermo Fisher Scientifics, Waltham, MA, USA). Cells were scrapped from the surfaces of the plates into microcentrifuge tubes and incubated 10 min in ice. A UP200s sonicator (Hielscher Ultrasonics GmbH, Teltow, Germany) was used to disrupt cell membranes for 10 s to release intracellular proteins. Cells were then centrifuged at 10,000 x g for 10 min at 4 ºC and the soluble protein fraction was collected. During this process, samples were always kept on ice to avoid protein degradation. Protein concentration was quantified by the Bradford method on a 96-well plate (Orange Scientific; Braine-l'Alleud, Belgium). A standard curve with known concentrations of bovine serum albumin (BSA, 0.125 to 2 µg/µL) was used to determine protein concentration. Samples were incubated with 200 µL of Bradford solution (Alfa Aesar, Ward Hill, MA, USA) for 5 min and then read at 595 nm. Samples were stored at -30ºC until use.

Western Blot (WB)

Protein extracts (30 µg) were mixed with 4x denaturing loading buffer (0.125 mM Tris pH 6.8; 4% sodium dodecyl sulphate (SDS), 20% glycerol, 10% β-mercaptoethanol, 0.004% bromophenol blue) and boiled for 5 min at 95 ºC, followed by incubation in ice for 5 min. Samples were separated by SDS-PAGE in 10% w/v acrylamide gels or in a gradient of 6% + 15% w/v acrylamide gels in running buffer (25 mM Tris-Base; 0,1% SDS; 190 mM Glycine) with a constant voltage of 120 V for 80 min. Five µL of NZYColour Protein Marker II (NZYTech) were used as molecular weight marker. Proteins were transferred to nitrocellulose membranes (Cytiva,

Marlborough, MA, USA) at 100 V for 1 h in transfer buffer (25 mM Tris-Base; 190 mM Glycine; 20% methanol). Membranes were stained with 0.1% w/v Ponceau S (Amresco, Solon, OH, USA) and 5% (v/v) acetic acid to confirm transfer efficiency. Ponceau S solution was washed with Tris-buffered saline (TBS, 150 mM NaCl; 50 mM Tris-base pH 7.4) with 0,05% Tween 20 (TBS-T). Then the membranes were blocked with 5% (w/v) non-fat dry milk in 1x TBS for 1 hour at room temperature. Membranes were washed with TBS-T (3x 10 minutes) and incubated with the corresponding primary antibody (Table 2) overnight at 4 ºC. Next day, membranes were washed with TBS-T (3x 10 minutes) and incubated with the corresponding secondary antibody (1:10000, Table 2) in blocking medium for 2 hours and washed with TBS-T (3x 10 minutes). Membranes were incubated with Pierce ECL Plus Western Blotting Substrate and imaged in an Amersham Imager 680 RGB.

Fluorescence Microscopy

C6 and C6 SACS-/- cells were incubated on coverslips in 24-well plates with 25 nM of Mitotracker Red CMXROS (Life technologies) for 25 min or with 75 µM of Mitoview Fix 640 (Biotium; Fremont, CA, USA) for 2h before cell fixing. Cells were washed with Dulbecco's Phosphate Buffered Saline (DPBS; San Marcos, TX, USA) and fixed with methanol for 15 min at -20ºC. Cells were then washed with DPBS (3 x 5 minutes) in agitation. Cell membranes were permeabilized by means of incubation with 0,1% Triton X-100 in DPBS for 10 minutes in agitation and then washed (3 x 5 minutes) with DPBS. Cells were then blocked with 1% BSA in DPBS-T for 1h in agitation at room temperature. Afterwards, incubation with primary antibodies (Table 2) was carried out overnight at 4ºC in a dark wet chamber. Cells were washed with DPBS for 5 minutes in the dark and incubated with the corresponding secondary antibodies (Table 2) for 2h at room temperature in a wet chamber. After washing off the secondary antibodies in DPBS, nuclei were counterstained with Hoechst 33342 (Molecular Probes, Willow Creek Rd Eugene, OR, USA). The coverslips were mounted on microscopy slides and imaged using a Leica TCS SPE Microscope, based on a Leica DMI4000B Microscope, in widefield mode. Imaging required immersion oil (RI 1.5180) used on the x64 objective HCX PL APO. The microscope was equipped with the detection device 1 PMT spectral (400-700nm) 1 transmitted light detector. Images were analyzed in ImageJ Fiji program[69].

Table 1 – Antibodies and their respective dilution and reference used in Western blot and Immunocytochemistry

Primary Anti-Bodies					
Antibody	**Dilution (for WB)**	**Dilution (for Microscopy)**	**Manufacture**	**City,Country**	**Reference**
Rabbit polyclonal anti-Sacsin	1:1000		MilliPore	Burlington, MA, USA	ABN1019
Mouse monoclonal anti-Sacsin (G3)	1:1000		Santa Cruz Biotechnology	Dallas, TX, USA	Sc-515118
Rabbit polyclonal anti-Glial Fibrillary Acid Protein (GFAP)	1:1000	1:200	MilliPore	Burlington, MA, USA	AB5804
Rabbit polyclonal anti-Glial Fibrillary Acid Protein (GFAP)	1:1000	1:200	Sigma-Aldrich	St. Louis, MO, USA	G9269
Mouse monoclonal anti-Glial Fibrillary Acid Protein (GFAP) (1.BB.807)		1:200	Santa Cruz Biotechnology	Dallas, TX, USA	sc-71143
Mouse monoclonal anti-Plectin (10F6)	1:1000		Santa Cruz Biotechnology	Dallas, TX, USA	Sc-33649
Mouse monoclonal anti-Vimentin (3CB2)	1:1000	1:200	Santa Cruz Biotechnology	Dallas, TX, USA	Sc-80975
Rabbit polyclonal anti-Vimentin	1:1000		Invitrogen	Waltham, MA, USA	PA5-2731
Mouse monoclonal anti-Nestin (Rat-401)	1:1000	1:200	Santa Cruz Biotechnology	Dallas, TX, USA	Sc-33677
Mouse monoclonal anti-STAT3 (F-2)	1:1000		Santa Cruz Biotechnology	Dallas, TX, USA	Sc-8019
Rabbit monoclonal anti-STAT3 (D3Z2G)	1:1000		Cell Signaling Technology	Dallas, TX, USA	#12640
Mouse monoclonal anti-phospho-STAT3 (Tyr705) (B-7)	1:1000		Santa Cruz Biotechnology	Dallas, TX, USA	Sc-8059
Rabbit polyclonal anti-acetyl-STAT3 (Lys49)	1:1000		St John's Laboratory	London, UK	STJ193228
Rabbit polyclonal anti-phospho-STAT3 (Ser727)	1:1000		Cell Signaling Technology	Danvers, MA, USA	#9134
Mouse monoclonal anti-GAPDH (6C5)	1:1000		Santa Cruz Biotechnology	Dallas, TX, USA	Sc-32233
Rabbit polyclonal anti-DDIT3/CHOP	1:1000		Abclonal	Wobum, MA, USA	A0221
Rabbit polyclonal anti-SMAD1	1:1000		Cell Signaling Technology	Danvers, MA, USA	#9743
Rabbit polyclonal anti-phospho-SMAD1 (Ser463/465)/ SMAD5 (Ser463/465)/ SMAD9 (Ser465/467) (D5B10)	1:1000		Cell Signaling Technology	Danvers, MA, USA	#13820

Secondary Antibodies					
Goat anti-mouse IgG (H+L)	1:10000		Thermo Fisher Scientifics	Waltham, MA, USA	A16066
Goat anti-rabbit IgG (H+L)	1:10000		Thermo Fisher Scientifics	Waltham, MA, USA	A16096
Goat anti-mouse IgG (H+L) Alexa Fluor Plus 657		1:800	Invitrogen	Waltham, MA, USA	A32728
Chicken anti-rabbit IgG (H+L) Alexa Fluor 594		1:800	Life technologies	Van Allen Way, CA, USA	A21442
Goat antt-mouse IgG (H+L) Alexa Fluor 546		1:800	Invitrogen	Waltham, MA, USA	A11003
Goat antt-rabbit IgG (H+L) Alexa Fluor 546		1:800	Invitrogen	Waltham, MA, USA	A11010

Data Analysis

Results were represented and analyzed with GraphPad Prism 5® software. Data were tested for normality by means of Shapiro-Wilk and Kolmogorov-Smirnov tests. Since they followed a normal distribution, they were analyzed by means of unpaired t-tests. Data were represented as the mean ± SD of at least 3 experiments unless otherwise indicated. Results were considered significant when $p \leq 0.05$.

Results

Deletion of sacsin in the C6 rat glioblastoma cell line

Several mouse and human cell lines were screened in advance for sacsin expression, and the results showed that primary rat astroglia and C6 rat glioblastoma cells expressed high levels of sacsin, as well as in the microglial N9 cells[70]. Due to the lack of research on the function of microglia and astroglia in ARSACS, the N9 microglial cell line and the C6 rat glioblastoma cell line were selected to produce sacsin knockout cells models. We tried to create N9 sacsin knockout cells clones as the first microglial model of ARSACS, but we failed due to persistent cell contaminations. However, sacsin knockout was successful in C6 cells, and this clone was established and published as a glial model of the ARSACS (Fernanda Murtinheira's PhD work). The deletion of sacsin in C6 SACS-/- cells was confirmed (Figure 6, p-value < 0.05) by western blot.

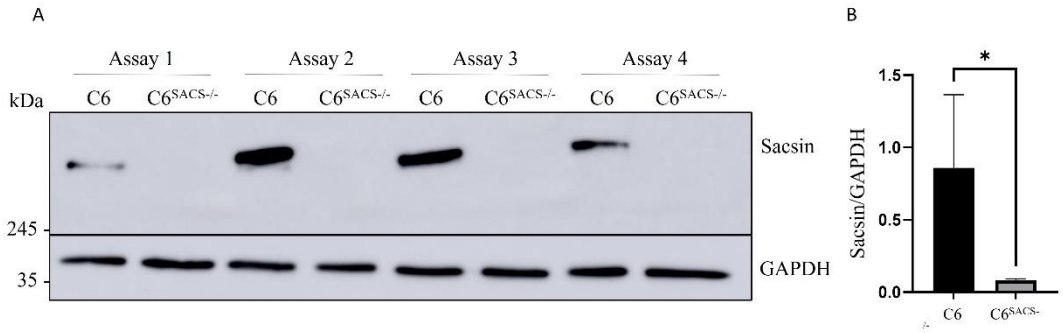

Figure 6 – Deletion of sacsin protein was successful. A) Representative image of a Western blot of reference C6 and C6 SACS-/- cells from four assays to confirm sacsin is present only in WT cells. **B)** Bands from the four assays (n=4) represented in the Western blot in A) were normalized with the respective GAPDH controls, quantified by densitometry and represented in the graphic. Data were analyzed by unpaired t-student test. Asterisks represent statistical significance: *, p-value<0,05.

Sacsin deletion alters organization Golgi apparatus

Sacsin is involved in intermediate filament distribution and organization, which in turn can disrupt the placement of organelles in neural cells, as described in previous studies. The expression of intermediate filaments can change in conditions of stress or inflammation. To analyze the response of IFs to inflammatory or stressful situations in the context of ARSACS in glial cells, both WT and SACS-/- C6 strains were subjected to serum starvation or incubation with IL-6/IL-6R and BMP-2 cytokines. Vimentin, GFAP and Nestin intermediate filaments had higher basal levels of expression in C6 Sacs-/- cells, compared to the reference C6 strain, maintaining this level of expression in starvation conditions (Figure 7A,7B) and after incubation with IL-6 and BMP-2 cytokines (Figure 7C,7D). However, the preliminary results of cytokine incubation show vimentin with an equally high expression in both sacs-/- and reference strains when treated with BMP-2 (Figure 7C). Although Nestin was expressed when incubated with the mentioned cytokines in SACS-/- cell strain, it had an higher expression level when the cells were induced with Il-6/IL-6R (Figure 7D). GFAP had an opposite effect, presenting higher levels when cells were incubated with BMP2, with or without IL-6/IL-6R incubation (Figure 7D). The expression levels of plectin, a protein that establishes cross-links between intermediate filaments to microtubules and actin filaments, was similar in both C6 and C6 SACS-/- cells in basal conditions (Figure 7E). The distribution of Nestin filaments was homogeneous in C6 WT cells, but they formed aggregates in the juxtanuclear position in C6 SACS-/- cells (Figure 7F). Vimentin and GFAP intermediate filaments were also analyzed but the result was not as clear due to overlap of fluorescence between the secondary antibody AlexaFluor 647 and Mitotracker or lack of specificity of the antibody or low quantity of vimentin present in the cells.

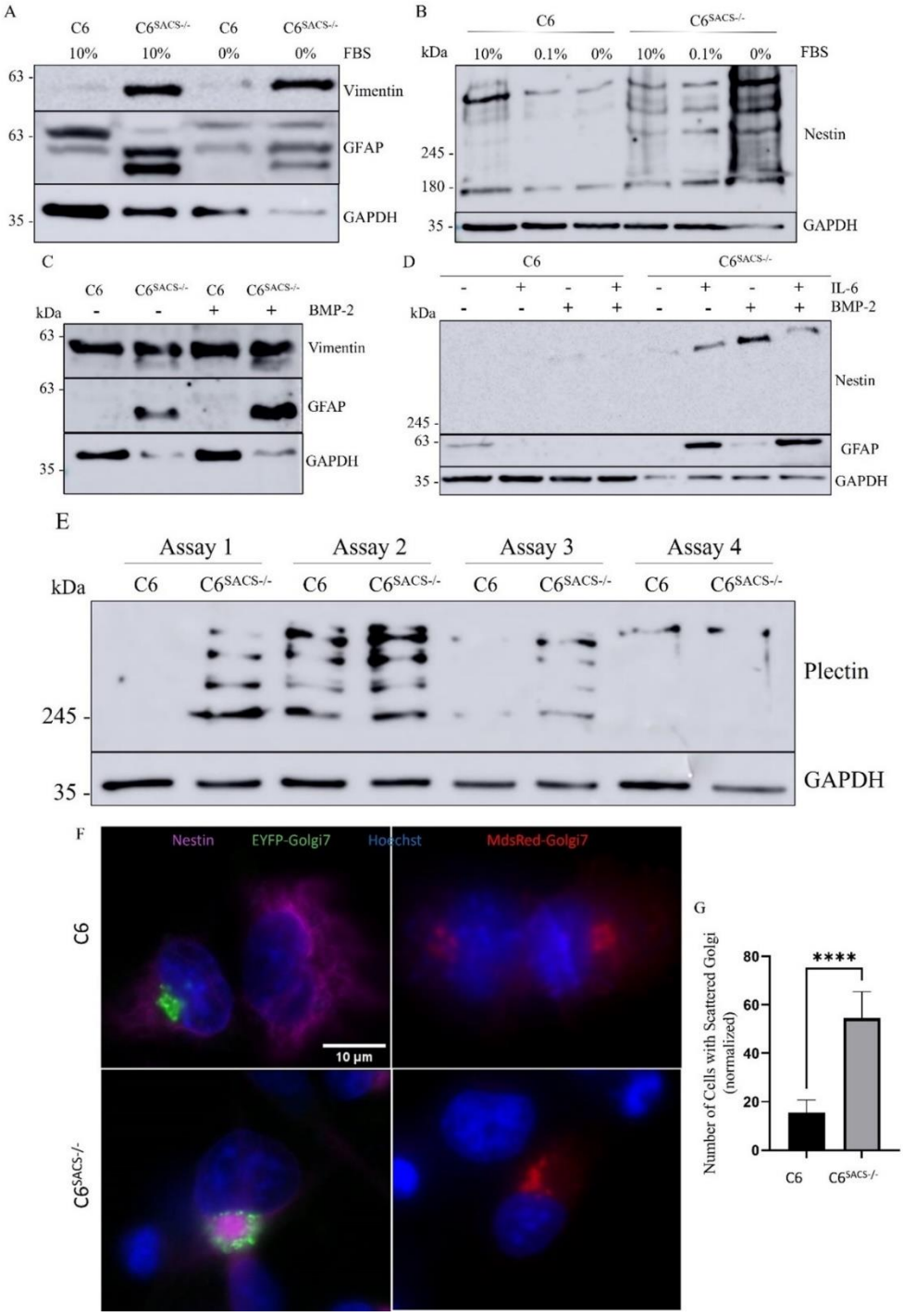

Figure 7 – Intermediate Filaments elevated expression and aggregation in the juxtanuclear position. A-B) C6 and C6 SACS-/- were subjected to complete medium (10% FBS) and serum starvation with 0 or 0.1% FBS for 24h. Representative western blot was analyzed with specific antibodies for Vimentin, GFAP, Nestin and GAPDH. C-D) C6 and C6 SACS-/- cells were incubated with IL-6/IL-6R and BMP-2 or just BMP-2 for 2h. Western blot analyzed with specific antibodies for Vimentin, GFAP, Nestin and GAPDH. E) Representative western Blot was analyzed with specific antibodies for Plectin and GAPDH for Plectin expression comparison between C6 and C6 SACS-/- cells. F) Golgi is found grouped next to the nucleus in C6 cells and scattered, around the Nestin aggregation in C6 SACS-/- cells. Representative microscopy images of C6 and C6 SACS-/- transfected with EYFP-Golgi7 (green) and MdsRed-Golgi7 (red) plasmids. Immunocytochemistry performed with antibodies specific for Nestin (magenta). After cell fixation, reference and SACS-/- C6 strains were incubated with Hoechst 33342 (blue) to observe the nucleus. Scale bar, 10µm. G) Cells with scattered Golgi were quantified and normalized versus the number of transfected cells in each assay (n=5, with 344 transfected reference C6 cells and 322 transfected SACS-/- cells). Statistical analysis was performed by normalitive tests followed by unpaired t-student test. Asterisks represent statistical significance: ****p-value<0,0001.

The organization of the Golgi apparatus was studied together with immunocytochemistry of IF proteins, in order to study the Golgi localization in relation with the IF aggregates. In C6 WT cells, the Golgi apparatus was usually assembled near the nucleus (Figure 7F). However, the Golgi apparatus is scattered in C6 SACS-/- cells, occasionally far from the nucleus (Figure 7F). Golgi often scattered around Nestin protein aggregates but was never localized inside IF aggregates. The number of C6 SACS-/- with scattered Golgi was significantly higher compared to C6 WT cells (Figure 7G).

Sacsin deletion disrupts the response of C6 cells to inflammatory cytokines and alters expression of S100B

Different protein signals are responsible for regulation of the inflammatory response in the brain: secretion of IL-6 and the alarmin S100B will enhance the inflammatory response on nearby cells while the BMP-2 cytokine has the opposite effect[52, 53]. Reference and SACS-/- C6 strains were incubated with pro-inflammatory cytokines IL-6 and its soluble receptor (IL-6R) for 20 min and 24h and the expression and activation of the downstream transcription factor STAT3 were analyzed. IL-6 was always co-incubated with IL-6R because previous work in Herrera´s lab (Mafalda Bragança's master thesis) demonstrated they were more effective at triggering the STAT3 pathway than IL-6 alone.

After 20 min and 24-hour incubation, there was an increase of phosphorylated STAT3 in tyrosine 705 (Y705) when incubated with IL-6/IL-6R in both control and knockout cells, but the increase was similar between the two cell lines, as shown in the preliminary results (Figure 8A). Acetylation in the residue lysine 49 (K49) was more prominent when the cells were incubated with IL-6/IL-6R. Moreover, there was a decrease in levels of expression, phosphorylation, or acetylation of STAT3 in SACS-/- strain after 24h (Figure 8A). Other cytokines were tested regarding their capacity of activation of the STAT3 cascade signaling in C6 cells. However, IL-11, IL-22, OSM, CNTF and IFN-α did not induce phosphorylation of STAT3 (Figure 8B). Besides, in this case, there was constant STAT3 expression even after 24h in both cell strains (Figure 8B).

SMAD1/5 and their activated/phosphorylated versions pSMAD1/5 are downstream BMP signaling and were used as additional indicators of the response of cells to inflammation-related cues. Reference and SACS-/- strains were incubated with IL-6/IL-6R and the anti-inflammatory cytokine BMP-2 for 20 min and 24h to study their response to these cytokines. There was an inconsistency of the levels of expression of SMAD1 between both C6 WT cell line and C6 SACS-/- cell line (Figure 9A) but 3 out the 4 assays SMAD1 had increase in reference C6 strain, which is the expected stated in a previous work (Mafalda Bragança, master thesis). SMAD1 and SMAD5 were only phosphorylated when the cells were incubated with BMP-2. There was higher increase of p-SMAD1/5 when induced by BMP-2 or both BMP2 and IL-6/IL-6R. However, there was no

phosphorylation when the cells were incubated solely by IL-6/IL-6R, suggesting that only BMP2 activates SMAD1 and SMAD5 phosphorylation.

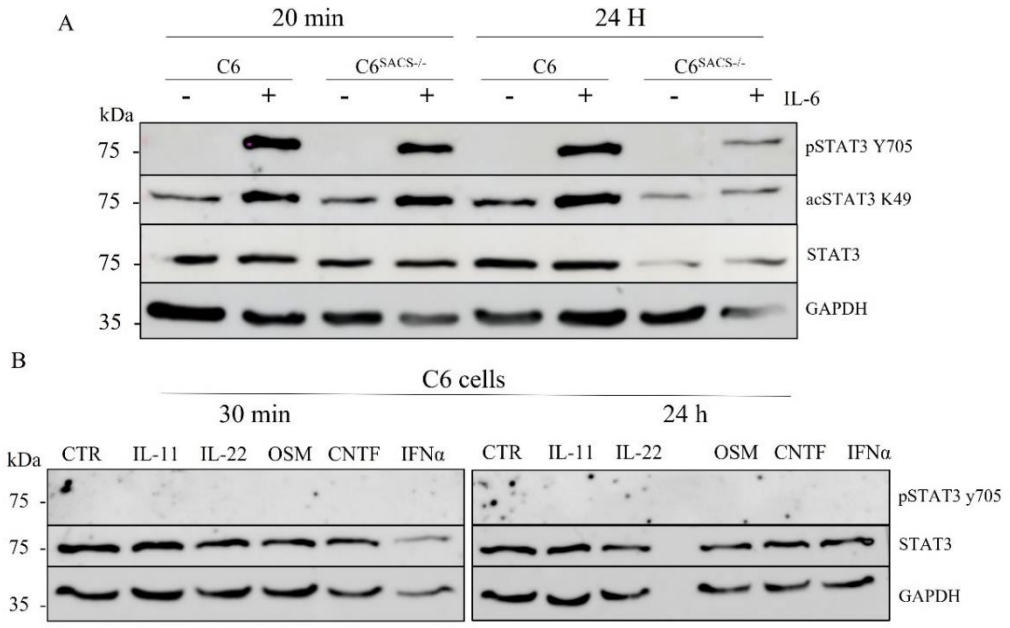

Figure 8 – Cytokine induction in STAT3 phosphorylation. IL-6 cytokine induced phosphorylation of STAT3 in C6 WT and C6 SACS-/- cells, while cytokines IL-11, IL-22, OSM, CNTF and IFNα did not activate STAT3. A) C6 and C6 SACS-/- cells were incubated with IL-6 (30ng/mL) and IL-6R (30ng/mL) for 20min and 24h. Representative western blot analyzed with specific antibodies for phosho-STAT3 (tyrosine 705, Y705), acetyl-STAT3 (Lysine 49, K49), STAT3 and GAPDH. B) Preliminary results of C6 cells when incubated with IL-11, IL-22, OSM, CNTF (30 ng/mL) and IFNα (100ng/mL) for 30min and 24h. Representative western blot was analyzed with specific antibodies for phoshp-STAT3 (tyrosine 705, Y705), STAT3 and GAPDH.

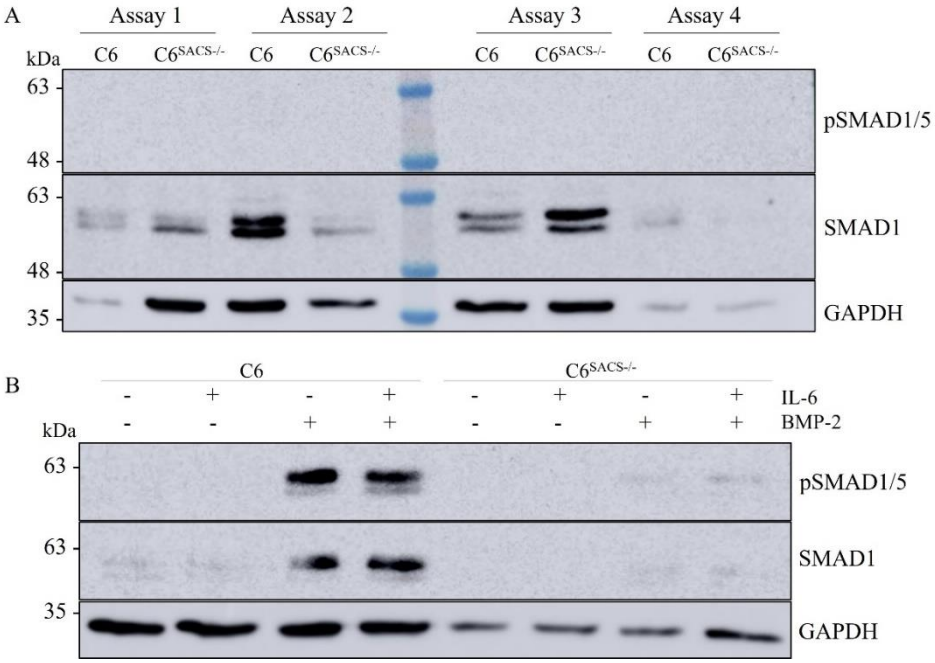

Figure 9– Activation of SMAD1/5 by BMP-2. BMP-2 cytokine induced phosphorylation of SMAD1/5 in C6 WT and C6 SACS-/- cells. A) Representative western blot analyzed with specific antibodies for phosphor-SMAD1/5, SMAD1 and GAPDH. B) C6 and C6 SACS-/- cells were incubated with IL-6/IL-6R and BMP-2 for 2h. Western blot analyzed with specific antibodies for phoshp-SMAD1/5, SMAD1 and GAPDH.

S100B is both an alarmin and a chaperone activated by astroglia during brain injury, triggering inflammation but also contributing to the elimination of pathological protein aggregates. The expression of the S100B protein is increased in C6 SACS-/- cells (Figure 10A) with a significant difference (Figure 10B) from the C6 WT cells, where there is no indication of expression of this protein.

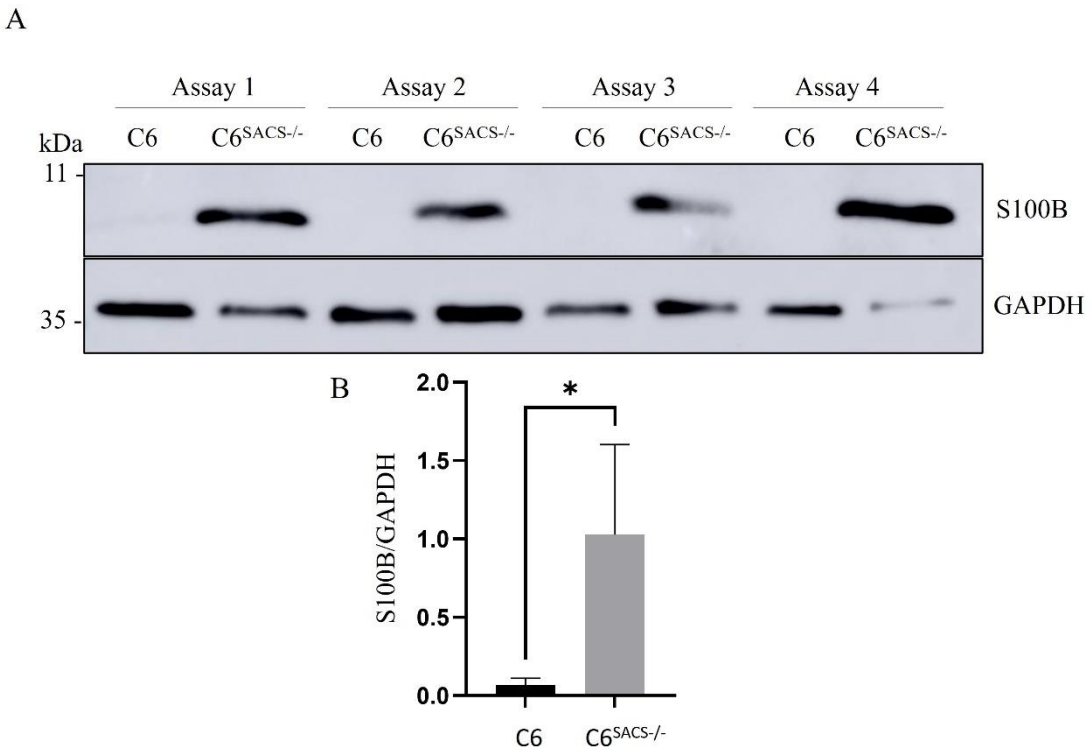

Figure 10 – S100B elevated expression in C6 SACS-/- cells. A) Representative western blot analyzed with specific antibodies of S100B and GAPDH to compare expression levels of S100B between reference C6 and SACS-/- strains. B) Bands from three of the four assays (n=3) represented in the Western blot in A) were normalized versus the respective GAPDH controls, quantified by densitometry and represented in the graphic. Statistical analysis was performed by normalitive tests followed by unpaired t-student test. Asterisks represent statistical significance: *p-value<0,05.

Sacsin deletion disrupts autophagy

Autophagy is essential for neuronal homeostasis, while its dysfunction has been directly linked to various neurodegenerative disorders. LC3, a protein that initiates Autophagosome formation when activated (LC3-II), was studied to determine whether loss of sacsin had any effect on autophagy. A higher level of expression of LC3 was observed in C6 SACS-/- cells, although non-significant. However, activated LC3-II can be observed with contradictory levels: higher in C6 WT in one assay, and higher in SACS-/- cells in other assays (Figure 11A).

C6 and C6 SACS-/- cells were transfected with LC3 fused with EGFP, which will be enriched in the membrane of early autophagosomes. EGFP is acid-sensitive and when the lysosomes fuse to autophagosomes the drop in pH will inhibit EGFP fluorescence. A higher number of green puncta

was observed in C6 WT cells, indicating a higher number of autophagosomes in reference C6 cells when compared to C6 SACS-/- cells (Figure 11A). Autophagosomes are usually distributed in the cell, not influenced by the IF aggregation in the juxtanuclear area in C6 SACS-/- cells (Figure 11B). There is a ≅0.4 fold decrease in autophagosomes in knockout cells (Figure 11C).

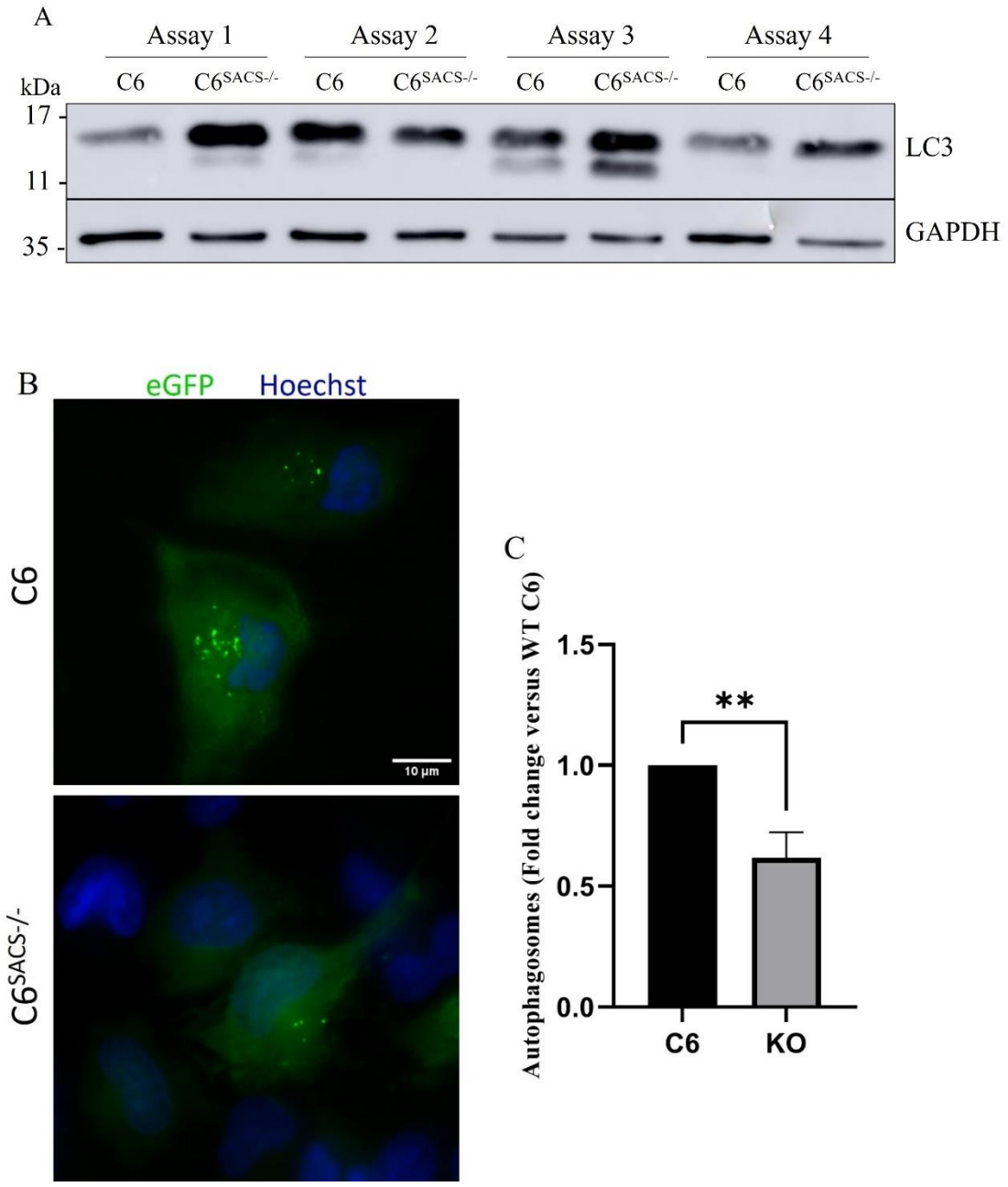

Figure 11 – Contradictory results of LC3. A) Representative western blot was analyzed with specific antibodies for LC3 and GAPDH comparing LC3-I (16-18 kDa) and LC3-II (14-16 kDa) expression on reference C6 and SACS-/- strains. B) Representative microscopy images reveal Autophagosomes (AP) green puncta and their distribution on reference C6 and SACS-/- strains. Reference C6 and SACS-/- strains were transfected with a plasmid that expressed LC3 conjugated with eGFP (green) and mCHERRY (red). After cell fixation, both cell lines were incubated with Hoechst 33342 (blue) to observe the nucleus. Scale bar, 10µm. C) Autophagosomes were quantified from reference C6 WT and SACS-/- strains and the ratio of total autophagosomes in reference C6 cells/ autophagosomes SACS-/- cells from each experiment (n=3) was calculated. Statistical analysis was performed by normalitive tests followed by unpaired t-student test. Asterisks represent statistical significance: **p-value=0,0034.

Sacsin deletion causes alterations in ER stress pathways

ER stress is one common hallmark in neurodegenerative diseases and a possible effect from the loss of sacsin in ARSACS cells[66, 67]. UPR is responsible for neutralizing ER stress by activating the transcription of various repair mechanisms but is also responsible for activating ER stress-induced apoptosis when repair is not possible[66]. The chaperone Bip is usually linked to stress signal receptors and detach from these receptors in stress conditions. The expression of Bip has no significant variation from reference C6 and SACS-/- strains, although a lower expression is found in starvation conditions in both cell strains (Figure 12A). ER stress-induced-apoptosis is mainly directed by the protein CHOP, which is the target for the next ER analysis. In normal conditions (10% FBS), CHOP is more expressed in C6 cells although there is still a very slight expression in C6 SACS-/- cells (Figure 12A). Moreover, a higher expression of CHOP is found in normal conditions than in starvation conditions (FBS 0%) (Figure 12A). The ER organization was also studied in fluorescent Microscopy experiments. ER-DsRed plasmid was transfected in both reference C6 and SACS-/- strains. There was similar ER distribution and organization in both reference C6 and SACS-/- strains (Figure 12B).

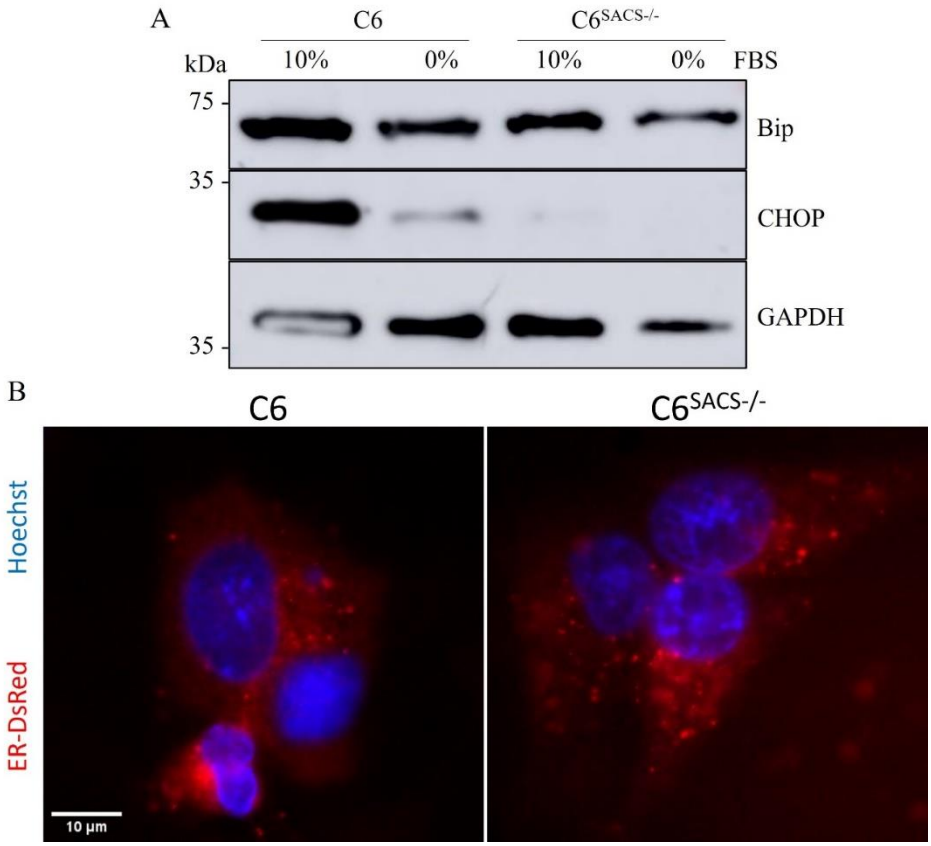

Figure 12 – Increase of CHOP expression in reference C6 and no change of Bip expression level, neither the positional changes in ER. A) reference C6 and SACS-/- strains were subjected to serum (10% FBS) for 24h. Representative western blot was analyzed with specific antibodies for Bip, CHOP and GAPDH. B) Representative microscopy images reveal no significant changes in ER organization in reference C6 or SACS-/- strains. reference C6 and SACS-/- strains were transfected with ER-DsRed (red) plasmid. After cell fixation, both cell lines were incubated with Hoechst 33342 (blue) to observe the nucleus. Scale bar, 10µm.

WFA partially mimics sacsin deletion effects on C6 cells

As stated in the literature, WFA directly binds to the conserved sequence of Vimentin present in Type III IF proteins, like GFAP, and disrupts the IF network. This disruption is similar to the phenotype seen in various cellular models of ARSACS. C6 cells were incubated with WFA at concentrations between 1-10µM. At a concentration of 2.5µM and above, there was a clear cell stress and induced death, distinguished by the smaller scale of nuclei and cells, and an abnormally scattered Golgi apparatus, mostly completely diffused throughout the whole cell Figure 13). At a concentration of 1µM of WFA, Nestin was found still well organized and, while not aggregated in the juxtanuclear position in an identical manner as in C6 SACS-/- cells, it was observed Nestin more concentrated around the nucleus (Figure 13). Golgi was scattered and far from the nucleus in all transfected cells (Figure 13).

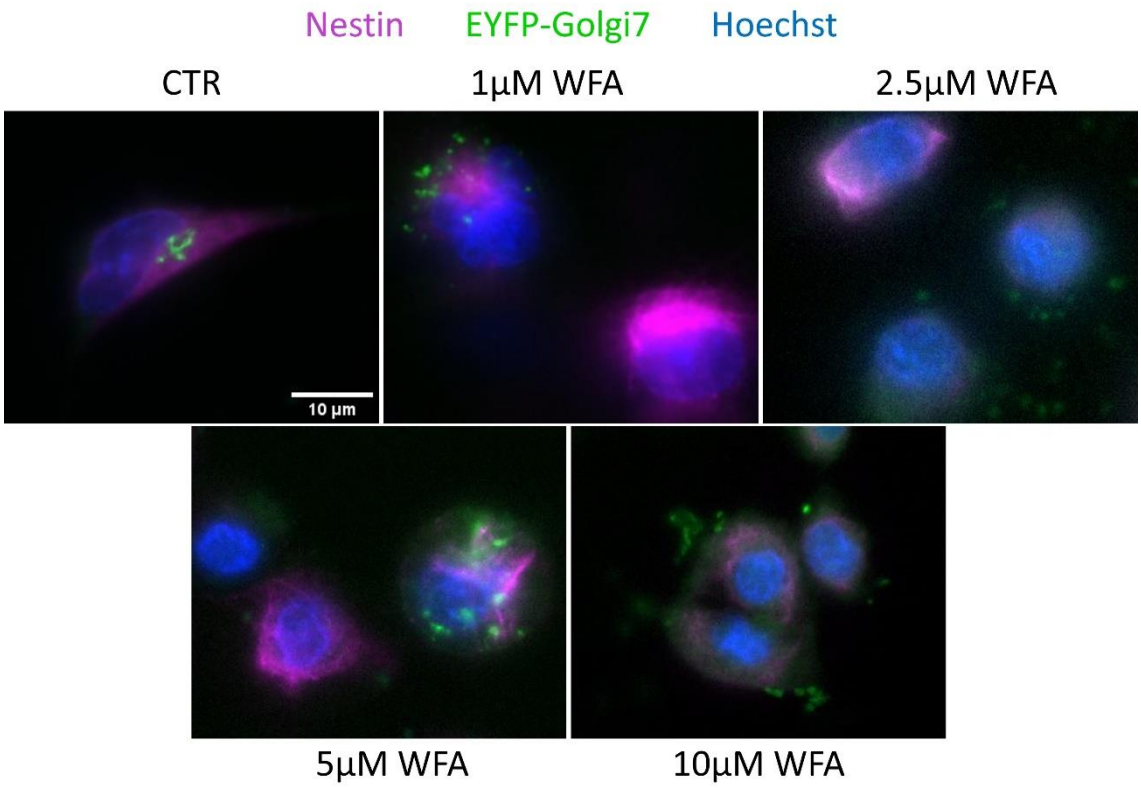

Figure 13 – WFA partially mimics sacsin deletion effects on C6 cells. A) Representative preliminary microscopy images reveal WFA effects on Nestin filaments and Golgi organization on reference C6 and SACS-/- strains. Reference C6 and SACS-/- strains were transfected with an EYFP-Golgi7 (green) plasmid, followed by immunocytochemistry with antibodies specific for Nestin (magenta) and secondary antibody AlexaFluor 647. After cell fixation, both cell lines were incubated with Hoechst 33342 (blue) to observe the nucleus. Scale bar, 10µm.

Discussion

This project focused on characterizing C6 SACS-/- cell line previously prepared by a previous work by Fernanda Murtinheira[70], through CRISPR-Cas9 knockout method as a glial cell model of the ARSACS neurodegenerative disease. Western blot of protein extracts from both C6 WT cell line and C6 SACS-/- cell line demonstrated that the CRISPR-Cas9 knockout was successful, showing sacsin bands only in reference C6 cells (Figure 6).

ARSACS studies demonstrated that loss of sacsin interfered with intermediate filament organization and distribution[2]. Western blot and immunocytochemistry studies confirmed an increased expression of Vimentin, GFAP (in WB) and Nestin IF proteins (in both WB and immunocytochemistry) and aggregation of Nestin in the juxtanuclear area in C6 SACS-/- cell line. This confirms that sacsin, probably via its chaperone domains activity, is involved in IF network organization.

The aggregation of IFs in the juxtanuclear area could interfere with the organization of organelles, such as the Golgi apparatus. While the Golgi apparatus is concentrated near the nucleus in C6 WT cells, in C6 SACS-/- cells the Golgi is found scattered around the IF protein aggregates in the juxtanuclear area (Figure 7F), sometimes farther from the nucleus. This is consistent with studies in ARSACS human dermal fibroblasts (HDFs), where Golgi was fragmented and scattered around vimentin aggregation in the juxtanuclear position[2], suggesting that Golgi is not only structurally altered in ARSACS fibroblasts, but also in SACS-/- astroglial cells. One common pathological characteristic in neurodegenerative diseases is the functional and structural alterations in Golgi apparatus: it suffers transformation into disconnected stacks, cisternae, tubules, and vesicles, resulting in Golgi membrane material loss and affecting the anterograde and retrograde transport in the early secretory pathway. These changes were reported from cellular models of Amyotrophic lateral sclerosis (ALS) and Parkinson, Huntington and Alzheimer's diseases[71, 72]. However, the underlying molecular mechanisms changes and their relevance to neurodegeneration is still unknown.

Besides intermediate filaments, a molecular characterization on neuroinflammation, autophagy and ER stress pathways was performed on SACS-/- C6 cells. Phosphorylation of STAT3 and its level of expression did not differ between the model and the control group when the cells were stimulated with IL-6/IL6R cytokines, although there was a decrease of activated or acetylated STAT3 or its expression in SACS-/- strain after 24 hours (Figure 8A). However, the increase of phosphorylated STAT3 after cytokine incubation was expected given that IL-6 activates the STAT3 pathway, which then causes STAT3 to be phosphorylated and migrate to the nucleus. However, hyperactivation of STAT3 is a common neurodegeneration feature. For instance, neuropathological investigations of AD patients and mice models showed an increase in phospho-

STAT3 Tyr705 in the hippocampus[73]. This indicates controversies between experiments and literature since it was expected an enhanced neuroinflammation and STAT3 activation. Moreover, there were similar levels of phosphorylation and acetylation of STAT3 after 20 min and 24 hours of exposure to cytokines. The suppressor of cytokine signaling 3 (SOCS3), a STAT3 inhibitor, is induced by tyrosine-phosphorylated STAT3 about 2h after IL-6 exposure[74], but a prolonged exposure to this cytokine leads to the association of IL-6R with the epidermal growth factor receptor (EGFR), which then activates STAT3 without being hindered by SOCS3[74]. This suggests that the 24-hour exposure to IL-6 should have induced an increased STAT3 phosphorylation. The lack of STAT3 activation may be influenced by sacsin chaperone activity or the increase in S100B expression, explained further ahead.

Reference C6 and SACS-/- strains incubated with both BMP2 and IL-6/IL-6R cytokines demonstrated phosphorylation of SMAD1/5 (Figure 9B). The intensity of activation was similar when incubated with only BMP2 and both cytokines. Moreover, when the cells were induced solely with the pro-inflammatory protein, there was no activation. This seems to suggest that IL-6/IL-6R does not influence SMAD activation nor interferes with BMP2 activity. However, Zhang, X. et al (2005) assessed IL-6's influence on TGF-1 signaling and established its mechanism[75]. When IL-6 was present, SMAD-responsive promoter (SBE)4-Lux activity was significantly more stimulated than when TGF-1 alone was used. Of TGF-1 receptors can be internalized by both caveolin-1 (Cav-1) lipid raft and early endosome antigen 1 (EEA-1) non-lipid raft-associated internalization[75]. Moreover, they found that IL-6 stimulation improved the trafficking of TGF-1 receptors to the non-lipid raft-associated pools, which led to greater TGF-1 SMAD signaling[75]. This study suggests that since BMP-2 belongs to the TGF-cytokine family, the SMAD pathway should be more activated when BMP-2 and IL-6/IL-6R are present.

S100B demonstrated higher expression levels in the SACS-/- cell line than the reference strain (Figure 10). S100B has an elevated expression in astrocytes in neurodegenerative diseases, and it is regarded as a marker for the diagnosis or prognosis of neurodegeneration[56]. This indicates that, as the other neurodegenerative diseases, ARSACS also shares the elevated S100B expression and can be a possible marker for ARSACS as well. This can be explained primarily by the high increase of intermediate filaments, because S100B is known to have chaperone activity and to help eliminate unfolded protein aggregates[58, 62]. The increased expression can also be explained by altered neuroinflammatory responses of sacsin-KO cells. Although neuroinflammation may decrease for SACS-/- strain after 24 hours, as seen in the preliminary results, S100B could be an indicator of inflammation in the knockout cells. However, S100B was found to inhibit IL-6 transcription, affecting the IL-6/STAT3 pathway[57]. This could be one of the factors preventing STAT3 from being significantly phosphorylated in C6 SACS-/- cells as compared to C6 WT.

Next, we focused on studying the autophagic system regarding the LC3 protein expression and distribution in cells with loss of sacsin. The expression of LC3 is maintained between the two cell lines in repeated assays, as seen in the Western Blot, but C6 WT cells had increased number of autophagosomes, represented as green puncta in the ICC microscopy images. The similar expression of LC3 between the control and sacsin knockout cells coincide with a previous report where LC3 expression was similar in control and ARSACS HDFs[2]. However, the study demonstrates an equal number of autophagosomes in both HDFs and ARSACS HDFs[2], contradicting the fold-decrease in autophagosomes we found in SACS-/- cells (Figures 11B, 11C). Cytosolic LC3 (LC3-I) is then conjugated to phosphatidylethanolamine (PE) catalyzed by enzymes Atg7 and Atg3[64] to form LC3-phosphatidylethanolamine conjugate (LC3-II) during the formation of autophagosomes[63–65]. The activated LC3-II levels are similar in both cell lines in the Western blot results, a similar outcome revealed from ARSACS HDFs by Duncan *et al* (2017)[2]. However, since there can be seen a higher number of autophagosomes in C6 cells in the ICC results, the activation of LC3-II should be higher in C6 WT cells in the Western blot analysis. However, Morani (2019) revealed a limited LC3-II expression in sacsin knockout cells when treated with FCCP (reversible inhibitor of mitochondrial oxidative phosphorylation), as opposed to the enhanced LC3-II expression in control SH-SY5Y neuroblastoma cells[76]. Moreover, sacsin-deficient cells showed reduced autophagosome accumulation and autophagosome-lysosome fusion, and additional inability of cargo degradation[76]. This suggests an autophagic flux defect in ARSACS cells, while confirming the reduced autophagosomes found in C6 SACS-/- cells.

In terms of LC3 distribution, the protein was dispersed through the cell, not apparently affected by the aggregation of the IF proteins in the juxtanuclear position in C6 SACS-/- cells. This contradicts this study by Duncan *et al* (2017) ultrastructural analysis of Human HDfs revealing autophagosomes and components of the autophagy–lysosome system, such as p62 and Lamp2 proteins intercepted in the vimentin aggregation[2]. Lysosomal-associated membrane protein 2 (Lamp2) are transmembrane proteins localized in lysosomes and are responsible for mediating lysosomal degradation of proteins[77], while ubiquitin-binding autophagic adaptor protein p62 is important for autophagic clearance of ubiquitinated proteins[78, 79]. This indicates that autophagosomes may have been localized in the IF aggregation in C6 SACS-/- cells.

Next, we focused on studying a possible phenotype regarding ER stress in cells with loss of sacsin. In starvation and microscopy experiments, levels of expression of Bip were similar in C6 WT and C6 SACS-/- cells. CHOP protein expression was higher in C6 control cells (Figure 12A). ER stress increases in starvation conditions due to metabolic and energetic stress[80]. This leads to induction of unfolded-protein response (UPR) to fight the ER stress, activated by the type-I transmembrane protein kinase, IRE1, and PKR-like endoplasmic reticulum kinase (PERK)[66, 67], increasing the CHOP expression and inducing ER stress apoptosis. The similar expression of Bip

in both C6 WT and C6 SACS-/- suggests that activation of IRE1 and PERK is not affected by the loss of sacsin, keeping a similar activity as WT cells. Higher CHOP expression in C6 WT indicate that loss of sacsin may interfere with expression of CHOP in knockout cells. One common feature in neurodegenerative disorders is the inducing ER stress due to accumulation and aggregation of unfolded proteins in the ER[66, 67], which contradicts the limited ER stress observed in C6 SACS-/- cells.

The study of ARSACS can be made via other methods, such as disruptive IF proteins reagents, such as WFA. Most experiments about WFA phenotype was studied on Nestin to directly compare with previous IF experiments on C6 SACS-/- cells. Nestin is still organized and distributed through the cell within C6 incubated with 1µM of WFA, a different phenotype from the juxtanuclear aggregation of Nestin in C6 SACS-/- cells (Figure 13). The IF filaments are disrupted to perinuclei aggregates in fibroblasts by WFA, via binding to Type III IF proteins such as vimentin and GFAP, which share the same intrinsic WFA binding domain[16]. Nestin is a type IV IF protein with a distinct constitution unsuitable for WFA binding and therefore not disrupting the Nestin network. However, although Nestin is more prominent during development, its expression is reinduced in mature cells during pathological situations, participating in the formation of glial scar after CNS injury[14]. Besides, Nestin co-polymerizes with type III IF vimentin, creating heterogeneous intermediate filaments[14, 81]. Although they are not aggregated, cells treated with 1µM of WFA exhibit greater fluorescence and a more condensed Nestin network when compared to the C6 control group. Besides IF proteins, the Golgi apparatus phenotype of WFA was also compared with Sacsin knockout cells. Golgi is found scattered in cells incubated with 1µM of WFA in a similar way to C6 SACS-/- cells (Figure 13). This shows WFA as a possible method of studying certain effects of IF type III aggregation in the cells, helping in turn in the study of C6 ARSACS model cells. This suggests that WFA may be fundamental tool for the study and characterization on sacsin and subsequent the ARSACS neurodegenerative disorder.

Conclusion

As expected, C6 SACS-/- cells demonstrated an increased intermediate filament expression and Nestin aggregation in the juxtanuclear area. A disruption of Golgi apparatus organization was also revealed, with the Golgi being scattered and normally surrounding the IF aggregation. IL-6/STAT3 and BMP2/SMAD pathways were not enhanced in sacsin deficient cells, suggesting that lack of sacsin may not respond to neuroinflammation or anti-inflammatory cues. Moreover, S100B expression is significantly higher in C6 SACS-/- cells. While LC3-I expression is similar in control and sacsin deficient cells, autophagosomes accumulation was reduced in C6 SACS-/- cell line, suggesting a decrease of autophagic flux in the absence of sacsin. Additionally, WFA partially mimicked the IF aggregation and Golgi dispersion found in SACS-/- cells. However, there were some contradictory results: there was no evidence of ER stress even in starvation

conditions, making it impossible to fully study the ER stress in SACS-/- cells. Our results indicate that there are further relevant alterations in glial cells lacking sacsin, and this could be relevant to ARSACS pathology and other pathologies related to alterations in IF networks.

Bibliography

1. Gentil BJ, Lai GT, Menade M, Larivière R, Minotti S, Gehring K, Chapple JP, Brais B, & Durham HD (2019) Sacsin, mutated in the ataxia ARSACS, regulates intermediate filament assembly and dynamics *FASEB J* **33(2)** 2982–2994, https://doi.org/10.1096/fj.201801556R.

2. Duncan EJ, Larivière R, Bradshaw TY, Longo F, Sgarioto N, Hayes MJ, Romano LEL, Nethisinghe S, Giunti P, Bruntraeger MB, Durham HD, Brais B, Maltecca F, Gentil BJ, & Chapple JP (2017) Altered organization of the intermediate filament cytoskeleton and relocalization of proteostasis modulators in cells lacking the ataxia protein sacsin *Hum Mol Genet* **26(16)** 3130–3143, https://doi.org/10.1093/hmg/ddx197.

3. Bouchard PA (2015) Characterizing the role of mitochondrial dysfunction in Autosomal Recessive Spastic Ataxia of Charlevoix- Saguenay (ARSACS) By .

4. Naef V, Marchese M, Ogi A, Fichi G, Galatolo D, Licitra R, Doccini S, Verri T, Argenton F, Morani F, & Santorelli FM (2021) Efficient neuroprotective rescue of sacsin-related disease phenotypes in zebrafish Int J Mol Sci, https://doi.org/10.3390/ijms22168401.

5. Kozlov G, Denisov AY, Girard M, Dicaire M-J, Hamlin J, McPherson PS, Brais B, & Gehring K (2011) Structural basis of defects in the sacsin HEPN domain responsible for autosomal recessive spastic ataxia of Charlevoix-Saguenay (ARSACS) *J Biol Chem* **286(23)** 20407–20412, https://doi.org/10.1074/jbc.M111.232884.

6. Grynberg M, Erlandsen H, & Godzik A (2003) HEPN: a common domain in bacterial drug resistance and human neurodegenerative proteins. *Trends Biochem Sci* **28(5)** 224–226, https://doi.org/10.1016/S0968-0004(03)00060-4.

7. Larivière R, Sgarioto N, Márquez BT, Gaudet R, Choquet K, McKinney RA, Watt AJ, & Brais B (2019) Sacs R272C missense homozygous mice develop an ataxia phenotype. *Mol Brain* **12(1)** 19, https://doi.org/10.1186/s13041-019-0438-3.

8. Wiche G (1998) Role of plectin in cytoskeleton organization and dynamics *J Cell Sci* **111(9)** 2477–2486, https://doi.org/10.1242/jcs.111.17.2477.

9. Wang N, & Stamenovic D (2002) Mechanics of vimentin intermediate filaments *J Muscle Res Cell Motil* **23(5–6)** 535–540, https://doi.org/10.1023/A:1023470709071.

10. Sanghvi-Shah R, & Weber GF (2017) Intermediate filaments at the junction of mechanotransduction, migration, and development *Front Cell Dev Biol* **5(SEP)** 1–19, https://doi.org/10.3389/fcell.2017.00081.

11. Middeldorp J, & Hol EM (2011) GFAP in health and disease *Prog Neurobiol* **93(3)** 421–443, https://doi.org/10.1016/j.pneurobio.2011.01.005.

12. Schnitzer J, Franke WW, & Schachner M (1981) Immunocytochemical demonstration of vimentin in astrocytes and ependymal cells of developing and adult mouse nervous system. *J Cell Biol* **90(2)** 435–447, https://doi.org/10.1083/jcb.90.2.435.

13. Gilyarov A V. (2008) Nestin in central nervous system cells *Neurosci Behav Physiol* **38(2)** 165–169, https://doi.org/10.1007/s11055-008-0025-z.

14. Consejería de Sanidad de la Comunidad Autónoma de Murcia (Spain) K, & Sociedad Española de Histología e Ingeniería Tisular. M (1986) *Histology and histopathology.* Gutenberg.

15. Petzold A (2015) Glial fibrillary acidic protein is a body fluid biomarker for glial pathology in human disease *Brain Res* **1600** 17–31, https://doi.org/https://doi.org/10.1016/j.brainres.2014.12.027.

16. Grin B, Mahammad S, Wedig T, Cleland MM, Tsai L, Herrmann H, & Goldman RD (2012) Withaferin A alters intermediate filament organization, cell shape and behavior *PLoS One* **7(6)** 1–13, https://doi.org/10.1371/journal.pone.0039065.

17. Gonatas NK, Stieber A, & Gonatas JO (2006) Fragmentation of the Golgi apparatus in neurodegenerative diseases and cell death *J Neurol Sci* **246(1–2)** 21–30, https://doi.org/10.1016/j.jns.2006.01.019.

18. Lowery J, Kuczmarski ER, Herrmann H, & Goldma RD (2015) Intermediate filaments play a pivotal role in regulating cell architecture and function *J Biol Chem* **290(28)** 17145–17153, https://doi.org/10.1074/jbc.R115.640359.

19. Gao YS, & Sztul E (2001) A novel interaction of the Golgi complex with the vimentin intermediate filament cytoskeleton *J Cell Biol* **152(5)** 877–893, https://doi.org/10.1083/jcb.152.5.877.

20. Martínez-Menárguez JÁ, Tomás M, Martínez-Martínez N, & Martínez-Alonso E (2019) Golgi fragmentation in neurodegenerative diseases: Is there a common cause? *Cells* **8(7)** 1–19, https://doi.org/10.3390/cells8070748.

21. Fan J, Hu Z, Zeng L, Lu W, Tang X, Zhang J, & Li T (2008) Golgi apparatus and neurodegenerative diseases *Int J Dev Neurosci* **26(6)** 523–534, https://doi.org/10.1016/j.ijdevneu.2008.05.006.

22. Matejuk A, & Ransohoff RM (2020) Crosstalk Between Astrocytes and Microglia: An Overview *Front Immunol* **11(July)** 1–11, https://doi.org/10.3389/fimmu.2020.01416.

23. Prinz M, Masuda T, Wheeler MA, & Quintana FJ (2021) Microglia and Central Nervous System-Associated Macrophages-From Origin to Disease Modulation. *Annu Rev Immunol* **39** 251–277, https://doi.org/10.1146/annurev-immunol-093019-110159.

24. Sousa C, Biber K, & Michelucci A (2017) Cellular and molecular characterization of microglia: A unique immune cell population Front Immunol, https://doi.org/10.3389/fimmu.2017.00198.

25. Sankowski R, Böttcher C, Masuda T, Geirsdottir L, Sagar, Sindram E, Seredenina T, Muhs A, Scheiwe C, Shah MJ, Heiland DH, Schnell O, Grün D, Priller J, & Prinz M (2019) Mapping microglia states in the human brain through the integration of high-dimensional techniques *Nat Neurosci* **22(12)** 2098–2110, https://doi.org/10.1038/s41593-019-0532-y.

26. Wang DD, & Bordey A (2008) The astrocyte odyssey. *Prog Neurobiol* **86(4)** 342–367, https://doi.org/10.1016/j.pneurobio.2008.09.015.

27. Dugger BN, & Dickson DW (2017) Pathology of Neurodegenerative Diseases. Cold Spring Harb Perspect Biol, https://doi.org/10.1101/cshperspect.a028035.

28. Kwon HS, & Koh SH (2020) Neuroinflammation in neurodegenerative disorders: the roles of microglia and astrocytes *Transl Neurodegener* **9(1)** 1–12,

https://doi.org/10.1186/s40035-020-00221-2.

29. Girard M, Larivière R, Parfitt DA, Deane EC, Gaudet R, Nossova N, Blondeau F, Prenosil G, Vermeulen EGM, Duchen MR, Richter A, Shoubridge EA, Gehring K, McKinney RA, Brais B, Chapple JP, & McPherson PS (2012) Mitochondrial dysfunction and Purkinje cell loss in autosomal recessive spastic ataxia of Charlevoix-Saguenay (ARSACS). *Proc Natl Acad Sci U S A* **109(5)** 1661–1666, https://doi.org/10.1073/pnas.1113166109.

30. Criscuolo C, Procaccini C, Meschini M, Cianflone A, Carbone R, Doccini S, Devos D, Nesti C, Vuillaume I, Pellegrino M, Filla A, De Michele G, Matarese G, & Santorelli F (2015) Powerhouse failure and oxidative damage in autosomal recessive spastic ataxia of Charlevoix-Saguenay J Neurol, https://doi.org/10.1007/s00415-015-7911-4.

31. Bagaria J, Bagyinszky E, & An SSA (2022) Genetics of Autosomal Recessive Spastic Ataxia of Charlevoix-Saguenay (ARSACS) and Role of Sacsin in Neurodegeneration Int J Mol Sci, https://doi.org/10.3390/ijms23010552.

32. Morani F, Doccini S, Chiorino G, Fattori F, Galatolo D, Sciarrillo E, Gemignani F, Züchner S, Bertini ES, & Santorelli FM (2021) Functional Network Profiles in ARSACS Disclosed by Aptamer-Based Proteomic Technology *Front Neurol* **11(January)** 1–8, https://doi.org/10.3389/fneur.2020.603774.

33. Lyman M, Lloyd DG, Ji X, Vizcaychipi MP, & Ma D (2014) Neuroinflammation: The role and consequences *Neurosci Res* **79** 1–12, https://doi.org/https://doi.org/10.1016/j.neures.2013.10.004.

34. DiSabato DJ, Quan N, & Godbout JP (2016) Neuroinflammation: the devil is in the details. *J Neurochem* **139 Suppl(Suppl 2)** 136–153, https://doi.org/10.1111/jnc.13607.

35. Erta M, Quintana A, & Hidalgo J (2012) Interleukin-6, a major cytokine in the central nervous system. *Int J Biol Sci* **8(9)** 1254–1266, https://doi.org/10.7150/ijbs.4679.

36. Yamasaki K, Taga T, Hirata Y, Yawata H, Kawanishi Y, Seed B, Taniguchi T, Hirano T, & Kishimoto T (1988) Cloning and expression of the human interleukin-6 (BSF-2/IFN beta 2) receptor. *Science* **241(4867)** 825–828, https://doi.org/10.1126/science.3136546.

37. Rose-John S (2012) IL-6 trans-signaling via the soluble IL-6 receptor: importance for the pro-inflammatory activities of IL-6. *Int J Biol Sci* **8(9)** 1237–1247, https://doi.org/10.7150/ijbs.4989.

38. Boulanger MJ, Chow D, Brevnova EE, & Garcia KC (2003) Hexameric structure and assembly of the interleukin-6/IL-6 alpha-receptor/gp130 complex. *Science* **300(5628)** 2101–2104, https://doi.org/10.1126/science.1083901.

39. Furtek SL, Backos DS, Matheson CJ, & Reigan P (2016) Strategies and Approaches of Targeting STAT3 for Cancer Treatment *ACS Chem Biol* **11(2)** 308–318, https://doi.org/10.1021/acschembio.5b00945.

40. Hillmer EJ, Zhang H, Li HS, & Watowich SS (2016) STAT3 signaling in immunity *Cytokine Growth Factor Rev* **31(713)** 1–15, https://doi.org/10.1016/j.cytogfr.2016.05.001.

41. Millot P, San C, Bennana E, Porte B, Vignal N, Hugon J, Paquet C, Hosten B, & Mouton-Liger F (2020) STAT3 inhibition protects against neuroinflammation and BACE1 upregulation induced by systemic inflammation. *Immunol Lett* **228** 129–134, https://doi.org/10.1016/j.imlet.2020.10.004.

42. Grundke-Iqbal I, Iqbal K, Tung YC, Quinlan M, Wisniewski HM, & Binder LI (1986)

Abnormal phosphorylation of the microtubule-associated protein tau (tau) in Alzheimer cytoskeletal pathology. *Proc Natl Acad Sci U S A* **83(13)** 4913–4917, https://doi.org/10.1073/pnas.83.13.4913.

43. Rothaug M, Becker-Pauly C, & Rose-John S (2016) The role of interleukin-6 signaling in nervous tissue. *Biochim Biophys Acta* **1863(6 Pt A)** 1218–1227, https://doi.org/10.1016/j.bbamcr.2016.03.018.

44. Huntley R, Jensen E, Gopalakrishnan R, & Mansky KC (2019) Bone morphogenetic proteins: Their role in regulating osteoclast differentiation. *Bone reports* **10** 100207, https://doi.org/10.1016/j.bonr.2019.100207.

45. Wang RN, Green J, Wang Z, Deng Y, Qiao M, Peabody M, Zhang Q, Ye J, Yan Z, Denduluri S, Idowu O, Li M, Shen C, Hu A, Haydon RC, Kang R, Mok J, Lee MJ, Luu HL, & Shi LL (2014) Bone Morphogenetic Protein (BMP) signaling in development and human diseases. *Genes Dis* **1(1)** 87–105, https://doi.org/10.1016/j.gendis.2014.07.005.

46. Massagué J, & Wotton D (2000) Transcriptional control by the TGF-beta/Smad signaling system. *EMBO J* **19(8)** 1745–1754, https://doi.org/10.1093/emboj/19.8.1745.

47. Wrana JL, & Attisano L (2000) The Smad pathway. *Cytokine Growth Factor Rev* **11(1–2)** 5–13, https://doi.org/10.1016/s1359-6101(99)00024-6.

48. Wu DH, & Hatzopoulos AK (2019) Bone morphogenetic protein signaling in inflammation *Exp Biol Med* **244(2)** 147–156, https://doi.org/10.1177/1535370219828694.

49. Lee H, Ueda M, Zhu X, Perry G, & Smith MA (2006) Ectopic expression of phospho-Smad2 in Alzheimer's disease: uncoupling of the transforming growth factor-beta pathway? *J Neurosci Res* **84(8)** 1856–1861, https://doi.org/10.1002/jnr.21072.

50. Nakashima K, Yanagisawa M, Arakawa H, Kimura N, Hisatsune T, Kawabata M, Miyazono K, & Taga T (1999) Synergistic signaling in fetal brain by STAT3-Smad1 complex bridged by p300. *Science* **284(5413)** 479–482, https://doi.org/10.1126/science.284.5413.479.

51. Yamamoto T, Matsuda T, Muraguchi A, Miyazono K, & Kawabata M (2001) Cross-talk between IL-6 and TGF-beta signaling in hepatoma cells. *FEBS Lett* **492(3)** 247–253, https://doi.org/10.1016/s0014-5793(01)02258-x.

52. Yoshimura A, Wakabayashi Y, & Mori T (2010) Cellular and molecular basis for the regulation of inflammation by TGF-β *J Biochem* **147(6)** 781–792, https://doi.org/10.1093/jb/mvq043.

53. Itoh Y, Saitoh M, & Miyazawa K (2018) Smad3–STAT3 crosstalk in pathophysiological contexts *Acta Biochim Biophys Sin (Shanghai)* **50(1)** 82–90, https://doi.org/10.1093/abbs/gmx118.

54. Kashima R, & Hata A (2018) The role of TGF-β superfamily signaling in neurological disorders *Acta Biochim Biophys Sin (Shanghai)* **50(1)** 106–120, https://doi.org/10.1093/abbs/gmx124.

55. Liu S, Tian Z, Yin F, Zhang P, W Y, Ding X, Wu H, Wu Y, Peng X, Yuan J, Qiang B, Fan W, & Fan M (2009) Expression and functional roles of Smad1 and BMPR-IB in glioma development. *Cancer Invest* **27(7)** 734–740, https://doi.org/10.1080/07357900802620786.

56. Steiner J, Bogerts B, Schroeter ML, & Bernstein HG (2011) S100B protein in neurodegenerative disorders *Clin Chem Lab Med* **49(3)** 409–424, https://doi.org/10.1515/CCLM.2011.083.

57. Alasady MJ, Terry AR, Pierce AD, Cavalier MC, Blaha CS, Adipietro KA, Wilder PT, Weber DJ, & Hay N (2021) The calcium-binding protein S100B reduces IL6 production in malignant melanoma via inhibition of RSK cellular signaling *PLoS One* **16(8 August)** 1–20, https://doi.org/10.1371/journal.pone.0256238.

58. Ziegler DR, Innocente CE, Leal RB, Rodnight R, & Gonçalves CA (1998) The S100B protein inhibits phosphorylation of GFAP and vimentin in a cytoskeletal fraction from immature rat hippocampus *Neurochem Res* **23(10)** 1259–1263, https://doi.org/10.1023/A:1020740115790.

59. Moreira GG, Cantrelle FX, Quezada A, Carvalho FS, Cristóvão JS, Sengupta U, Puangmalai N, Carapeto AP, Rodrigues MS, Cardoso I, Fritz G, Herrera F, Kayed R, Landrieu I, & Gomes CM (2021) Dynamic interactions and Ca2+-binding modulate the holdase-type chaperone activity of S100B preventing tau aggregation and seeding *Nat Commun* **12(1)** 1–16, https://doi.org/10.1038/s41467-021-26584-2.

60. Cristóvão JS, Figueira AJ, Carapeto AP, Rodrigues MS, Cardoso I, & Gomes CM (2020) The S100B alarmin is a dual-function chaperone suppressing amyloid-β oligomerization through combined zinc chelation and inhibition of protein aggregation *ACS Chem Neurosci* **11(17)** 2753–2760, https://doi.org/10.1021/acschemneuro.0c00392.

61. Kleindienst A, Hesse F, Bullock MR, & Buchfelder M (2007) The neurotrophic protein S100B: value as a marker of brain damage and possible therapeutic implications *Prog Brain Res* **161** 317–325, https://doi.org/10.1016/S0079-6123(06)61022-4.

62. Garbuglia M, Verzini M, & Donato R (1998) Annexin VI binds S100A1 and S100B and blocks the ability of S100A1 and S100B to inhibit desmin and GFAP assemblies into intermediate filaments *Cell Calcium* **24(3)** 177–191, https://doi.org/https://doi.org/10.1016/S0143-4160(98)90127-0.

63. Huang R, & Liu W (2015) Identifying an essential role of nuclear LC3 for autophagy *Autophagy* **11(5)** 852–853, https://doi.org/10.1080/15548627.2015.1038016.

64. Tanida I, Ueno T, & Kominami E (2008) LC3 and autophagy *Methods Mol Biol* **445(2)** 77–88, https://doi.org/10.1007/978-1-59745-157-4_4.

65. Corti O, Blomgren K, Poletti A, & Beart PM (2020) Autophagy in neurodegeneration: New insights underpinning therapy for neurological diseases *J Neurochem* **154(4)** 354–371, https://doi.org/10.1111/jnc.15002.

66. Oyadomari S, & Mori M (2004) Roles of CHOP/GADD153 in endoplasmic reticulum stress *Cell Death Differ* **11(4)** 381–389, https://doi.org/10.1038/sj.cdd.4401373.

67. Bertolotti A, Zhang Y, Hendershot LM, Harding HP, & Ron D (2000) Dynamic interaction of BiP and ER stress transducers in the unfolded-protein response *Nat Cell Biol* **2(6)** 326–332, https://doi.org/10.1038/35014014.

68. Estébanez B, De Paz JA, Cuevas MJ, & González-Gallego J (2018) Endoplasmic reticulum unfolded protein response, aging and exercise: An update *Front Physiol* **9(December)** 1–9, https://doi.org/10.3389/fphys.2018.01744.

69. Schneider CA, Rasband WS, & Eliceiri KW (2012) NIH Image to ImageJ: 25 years of image analysis *Nat Methods* **9(7)** 671–675, https://doi.org/10.1038/nmeth.2089.

70. Murtinheira F, Migueis M, Letra-Vilela R, Diallo M, Quezada A, Valente CA, Oliva A, Rodriguez C, Martin V, & Herrera F (2022) Sacsin Deletion Induces Aggregation of Glial Intermediate Filaments Cells, https://doi.org/10.3390/cells11020299.

71. Nakagomi S, Barsoum MJ, Bossy-Wetzel E, Sütterlin C, Malhotra V, & Lipton SA (2008) A Golgi fragmentation pathway in neurodegeneration *Neurobiol Dis* **29(2)** 221–231, https://doi.org/10.1016/j.nbd.2007.08.015.

72. Rabouille C, & Haase G (2016) Editorial: Golgi Pathology in Neurodegenerative Diseases *Front Neurosci* **9(January)** 2015–2017, https://doi.org/10.3389/fnins.2015.00489.

73. Wan J, Fu AKY, Ip FCF, Ng H-K, Hugon J, Page G, Wang JH, Lai K-O, Wu Z, & Ip NY (2010) Tyk2/STAT3 signaling mediates beta-amyloid-induced neuronal cell death: implications in Alzheimer's disease. *J Neurosci Off J Soc Neurosci* **30(20)** 6873–6881, https://doi.org/10.1523/JNEUROSCI.0519-10.2010.

74. Wang Y, van Boxel-Dezaire AHH, Cheon H, Yang J, & Stark GR (2013) STAT3 activation in response to IL-6 is prolonged by the binding of IL-6 receptor to EGF receptor. *Proc Natl Acad Sci U S A* **110(42)** 16975–16980, https://doi.org/10.1073/pnas.1315862110.

75. Xiao LZ, Topley N, Ito T, & Phillips A (2005) Interleukin-6 regulation of transforming growth factor (TGF)-β receptor compartmentalization and turnover enhances TGF-β1 signaling *J Biol Chem* **280(13)** 12239–12245, https://doi.org/10.1074/jbc.M413284200.

76. Morani F, Doccini S, Sirica R, Paterno M, Pezzini F, Ricca I, Simonati A, Delledonne M, & Santorelli FM (2019) Functional Transcriptome Analysis in ARSACS KO Cell Model Reveals a Role of Sacsin in Autophagy *Sci Rep* **9(1)** 1–16, https://doi.org/10.1038/s41598-019-48047-x.

77. Hubert V, Peschel A, Langer B, Gröger M, Rees A, & Kain R (2016) LAMP-2 is required for incorporating syntaxin-17 into autophagosomes and for their fusion with lysosomes. *Biol Open* **5(10)** 1516–1529, https://doi.org/10.1242/bio.018648.

78. Nezis IP, Simonsen A, Sagona AP, Finley K, Gaumer S, Contamine D, Rusten TE, Stenmark H, & Brech A (2008) Ref(2)P, the Drosophila melanogaster homologue of mammalian p62, is required for the formation of protein aggregates in adult brain. *J Cell Biol* **180(6)** 1065–1071, https://doi.org/10.1083/jcb.200711108.

79. Komatsu M, Waguri S, Koike M, Sou Y-S, Ueno T, Hara T, Mizushima N, Iwata J-I, Ezaki J, Murata S, Hamazaki J, Nishito Y, Iemura S-I, Natsume T, Yanagawa T, Uwayama J, Warabi E, Yoshida H, Ishii T, Kobayashi A, Yamamoto M, Yue Z, Uchiyama Y, Kominami E, & Tanaka K (2007) Homeostatic levels of p62 control cytoplasmic inclusion body formation in autophagy-deficient mice. *Cell* **131(6)** 1149–1163, https://doi.org/10.1016/j.cell.2007.10.035.

80. Albers E, Larsson C, Andlid T, Walsh MC, & Gustafsson L (2007) Effect of nutrient starvation on the cellular composition and metabolic capacity of Saccharomyces cerevisiae. *Appl Environ Microbiol* **73(15)** 4839–4848, https://doi.org/10.1128/AEM.00425-07.

81. Chou Y-H, Khuon S, Herrmann H, & Goldman RD (2003) Nestin promotes the phosphorylation-dependent disassembly of vimentin intermediate filaments during mitosis. *Mol Biol Cell* **14(4)** 1468–1478, https://doi.org/10.1091/mbc.e02-08-0545.